


Article

Impact of Recycled Concrete and Brick Aggregates on the Flexural and Bond Performance of Reinforced Concrete

Abdul Basit¹, Rashid Hameed¹, Safer Abbas¹, Muhammad Shoaib Karam², Shaban Shahzad¹,
Syed Minhaj Saleem Kazmi^{3,*}  and Muhammad Junaid Munir^{3,*} 

¹ Civil Engineering Department, University of Engineering and Technology, Lahore 54890, Pakistan; abdulbasit4676@gmail.com (A.B.); rashidmughal@uet.edu.pk (R.H.); safer.abbas@uet.edu.pk (S.A.); shaban.shahzad12@gmail.com (S.S.)

² Department of Civil Engineering, University of Engineering and Technology, Lahore, Narowal Campus, Narowal 51601, Pakistan; shoaib.karam@uet.edu.pk

³ Guangdong Provincial Key Laboratory of Durability for Marine Civil Engineering, Shenzhen University, Shenzhen 518060, China

* Correspondence: minhajkazmi17@gmail.com (S.M.S.K.); junaidmunir17@gmail.com (M.J.M.)

Abstract: The construction industry strongly relies on concrete and clay bricks for various applications. The escalating demand for these materials, driven by rapid population growth, has led to resource depletion and increased construction and demolition waste (CDW). Recycling CDW into construction materials, particularly in the form of recycled concrete aggregates (RCAs) and recycled brick aggregates (RBAs), has emerged as a promising solution. This study deals with the structural performance of concrete incorporating RCAs and RBAs. The experimental program encompasses material characterization, concrete mix design, and several tests to assess density, compressive strength, bond behavior, and flexural properties. The results indicate that the replacement of fine natural aggregate (NA) with fine RCAs or RBAs has a negligible impact on density, while the partial replacement of coarse NAs with RAs yields modest reductions in compressive strength. Notably, the bond strength between steel rebar and concrete is influenced by the type and content of RA, with specimens containing RCAs exhibiting a higher bond strength than those with RBAs. Empirical models used to predict bond strength generally align with experimental results, with conservative predictions by some models, such as ACI 318, and overestimation by others, such as models proposed by AS-3600 and CEB-FIB. The flexural tests of beams highlight the variation in stiffness and load-bearing capacity with the proportion of NAs replaced by RAs. While beams with 50% NA replacement demonstrate comparable performance to control beams, those with 100% RA replacement exhibit lower cracking and yielding stiffness. Cracking patterns in beams with RAs differ from control beams, with RA-containing beams showing more cracks and an altered crack distribution. The findings underscore the feasibility of using recycled aggregates in construction, with partial NA replacement offering a balance between sustainable material usage and desired structural properties.

Keywords: reinforced concrete; recycled aggregates; bond strength; flexural performance; sustainable practice



Citation: Basit, A.; Hameed, R.; Abbas, S.; Karam, M.S.; Shahzad, S.; Kazmi, S.M.S.; Munir, M.J. Impact of Recycled Concrete and Brick Aggregates on the Flexural and Bond Performance of Reinforced Concrete. *Appl. Sci.* **2024**, *14*, 2719. <https://doi.org/10.3390/app14072719>

Academic Editor: Kang Su Kim

Received: 19 February 2024

Revised: 14 March 2024

Accepted: 21 March 2024

Published: 24 March 2024



Copyright: © 2024 by the authors. Licensee MDPI, Basel, Switzerland. This article is an open access article distributed under the terms and conditions of the Creative Commons Attribution (CC BY) license (<https://creativecommons.org/licenses/by/4.0/>).

1. Introduction

Concrete and burnt-clay bricks are the most widely used construction materials on the globe [1,2]. Each year, about 14 billion cubic meters of concrete are produced for various applications such as transportation infrastructure, residential and commercial buildings, and large structures such as dams [3]. Similarly, around 1400–1500 billion units of clay bricks are produced every year, and 87% of the total production of burnt-clay bricks is contributed by Asian countries, with the largest contributions from China, India, and Pakistan, respectively [4,5]. With the exponential growth in population, the use of solid

clay bricks and concrete for construction is increasing rapidly, resulting in the depletion of natural resources being utilized in the production of these materials. Along with the increasing demand for the construction of infrastructure to fulfill the needs of an ever-increasing population, a constant increase in construction and demolition waste (CDW) is observed all over the world because of several contributing factors. For example, many existing, aged concrete structures are being dismantled and reconstructed in order to meet new design and specification requirements [6]. Moreover, restoration or replacement of deteriorated infrastructure, urban re-development, and natural disasters, for instance, floods, tsunamis, and earthquakes, have contributed to the vast accumulation of CDW. For instance, around 19 million tons of CDW were generated due to the 2015 Nepal earthquake within a few days [7]. Similarly, according to the reports, a recent earthquake in Türkiye resulted in the accumulation of around 104 million tons of CDW [8]. The most popular way to dispose of such construction waste is by dumping it in landfills. However, landfills have been overburdened as a result of the uncontrolled disposal of CDW, posing environmental risks. As a result, the researchers are working to find the best way to effectively manage such massive CDW and to protect against the depletion of non-renewable natural aggregates. One of the solutions proposed by the researchers is to recycle CDW and use it as aggregate in fresh concrete [9–13].

Various research studies in the recent time [14–19] have been performed to evaluate the durability and mechanical performance of recycled-aggregate concrete (RAC) and their performance evaluation and suitability to manufacture un-reinforced concrete elements such as bricks, concrete pavers [9–11], slabs without shear reinforcement [20], piloti-type structures [21], and pavements in expressways [22]. Similarly, numerous experimental investigations were carried out to examine the flexural performance and shear strength predictions [23–25] of reinforced RAC by using it in structural elements [26–30]. However, research work on the structural performance of concrete with high or complete replacement of natural aggregates (NA) by recycled concrete aggregates (RCAs) and recycled brick aggregates (RBAs) is limited. In general, RAC can exhibit the same strength and serviceability characteristics as conventionally reinforced concrete [31–33]. Meng et al. [34] investigated the failure process of mixed recycled aggregate concrete under the influence of brick aggregates, and they reported that for such concrete, increased content of aggregates produced from waste bricks and impurities caused an enhancement of the deformability and evident volume changes. Dang et al. [35] studied the impact of the morphological characteristics and pore structure of recycled fine aggregates derived from clay bricks on the mechanical properties of concrete using SEM. It was noticed that the complex surface morphology of these aggregates improved the splitting tensile strength and exhibited greater mechanical interlocking of the ITZ than the fine NA. To stimulate its usage as structural concrete, however, it was found necessary to design RC members manufactured from recycled coarse aggregates using current design procedures. Therefore, more full-scale research was recommended to be conducted for an in-depth understanding of the structural performance of such composites.

The usefulness of structural concrete (RC) is derived from the combined action of reinforcing rebars and concrete. Load transfer must occur between these two materials to ensure composite action. In this regard, force transfer from rebars to concrete or from concrete to steel rebars will only be effective if a good bond exists between both materials [36]. Therefore, one of the important factors in the design of RC structures is the bond behavior between steel reinforcing bars and concrete. Extensive research work has been conducted over the past many decades on the bond stress–slip response of natural aggregate concrete (NAC) and steel reinforcing deformed bars, and bond strength for such composites has already been formulated and quantified [37–41]. However, very limited literature is found dealing with the bond stress–slip response of steel reinforcing bars and RAC containing RCAs and/or RBAs. Prince and Singh [42] conducted pull-out tests to examine the bond behavior between steel rebar and RAC. They prepared RAC by replacing the coarse NAs with coarse RCAs at replacement levels of 0, 25, 50, 75, and 100%. From

the findings of this study, they concluded that the relative bond strength of RAC prepared with coarse RCAs was higher. Compared to concrete prepared with full NA, the maximum bond strength was obtained at a replacement level of 100%. Likewise, Zheng and Xiao [43] investigated the bond–slip performance of ordinary recycled brick-aggregate (RBA) concrete, considering the replacement ratio from 0% to 100% with an increment of 25% as the primary varying parameter for 40 pull-out specimens. They found that as the replacement ratio of RBAs varied from 0% up to 50% and then up to 100%, the decrease in the bond strength was 19.91–28.11% and 46.32–49.63%, respectively, corresponding to different embedment lengths. Another study was conducted by Zhang et al. [44] to analyze the bond behavior between steel and RAC in slabs. Test specimens were prepared by replacing the coarse NAs with coarse RCAs at 0, 50, and 100% replacement levels. They observed a 4–20% decrease in the ultimate bond strength and an 8–14% decrease in the stiffness in the presence of RCAs in the concrete. Hoque et al. [45] analyzed the bond response between concrete incorporating RBAs as coarse aggregates and steel rebar. Based on the experimentation, they developed an analytical model to calculate the bond strength of brick aggregate concrete (BAC). Moreover, they found that BAC exhibited a higher bond strength compared to that predicted using the model proposed by ACI 318 [46] for stone aggregate concrete. The factors that affect the bond strength include reinforcement size and geometry, rebar position, bonded length, amount of transverse reinforcement, concrete strength, and thickness of concrete cover [47–49]. Since the concrete strength is altered by replacing NAs with RCAs or RBAs [50–52], experimental investigation is required to assess the impact of fine and coarse RCAs and/or RBAs on the bond properties to avoid underestimation of bond strength, which may lead to financial losses, or overestimation, which may lead to failure.

Keeping in view the structural performance of reinforced RAC and its real application in concrete structures, the investigation of its flexural behavior is of great significance. Visintin et al. [26] studied the flexure performance of multi-generation recycled concrete beams. Three different generations (RA-1, RA-2, and RA-3) were used to prepare RAC. In the RA-1 generation, RCAs were produced by crushing virgin aggregate concrete, while in the RA-2 generation, RCAs were produced by crushing RA-1 concrete. Similarly, in the RA-3 generation, RCAs were produced by crushing RA-2 concrete. RC beams were cast and tested under four-point bending loading. It was noticed that the flexural response of an under-reinforced RC beam was controlled by the yielding of steel, and a slight increase in ductility was noticed because of the reduced interlocking of recycled aggregates. The reduction in beam stiffness was observed with the increase in the recycling of aggregates because of the degradation in the concrete elastic modulus and tensile strength. Momeni et al. [53] analyzed the flexure performance of RC beams of 200 mm × 300 mm × 1500 mm size constructed using natural and recycled aggregates. A 10% reduction in the ultimate flexural strength was reported for RAC beams as compared to those prepared using NAC. Similarly, the flexural behavior of reinforced RAC beams was investigated by Ignjatovic et al. [54]. They prepared RC beams by replacing 0%, 50%, and 100% coarse NAs with coarse RCAs and were subjected to four-point bending tests. Their study concluded that with the same reinforcement ratios, a slight difference in the failure load was observed for reinforced RAC beams. Further, the amount of coarse recycled aggregate in the concrete had a large influence on the size of the failure surface and the severity of concrete degradation at the flexural failure of the beam. They found that the size of the failure surface and severity of concrete disintegration increased as the recycled aggregate content increased. Although some past studies showed a positive impact of fine RCAs and RBAs on the properties of sustainable mortar and concrete [55–57], a literature review revealed that there is no research that specifically highlights the effect of fine RCAs or fine RBAs on the flexural response of RC structural members. Therefore, an experimental investigation is required to assess the influence of fine RCAs or fine RBAs on the properties of reinforced RAC.

In this context, the present study aimed to investigate the impact of fine and coarse recycled concrete and brick aggregates on the bond and flexural performance of reinforced

concrete. Four-point flexure tests were performed to study the flexural response, while the bond performance was assessed by carrying out direct pull-out testing. A comparison of bond strength predicted by various equations proposed in the literature and experimentally obtained values in this study has also been presented in this contribution. The bond and flexural performance of RAC made using RCAs or RBAs is compared with the performance exhibited by NAC. A total of thirteen concrete mixes, including one control mix, were prepared and used to cast specimens of pull-out tests and RC beams. All concrete mixes were also tested to determine their strength in compression.

2. Experimental Program

2.1. Materials

Two types of aggregates were investigated in this study: RCAs and RBAs. Concrete compositions were prepared by 100% replacement of fine natural aggregates (Nas) with fine RCAs or fine RBAs and partial/full replacement of coarse Nas with coarse RCAs or coarse RBAs. For comparison, the control mix was also prepared with 100% NAs (both fine and coarse).

RCAs were produced by crushing broken samples (cubes and cylinders) of concrete with a compressive strength ranging from 21 to 28 MPa, while RBAs were prepared by crushing old bricks with a compressive strength greater than 10.5 MPa. Chunks of waste concrete and old, damaged bricks were initially broken into large pieces using manual hammering and then passed through the roller crushers. The crushed material was finally sieved in order to separate fine and coarse aggregate fractions. The procedure for producing both types of recycled aggregates is described in Figure 1. Various tests were performed following ASTM/BS standards to determine the physical and mechanical properties of NA, RCAs, and RBAs. The results are presented in Table 1.

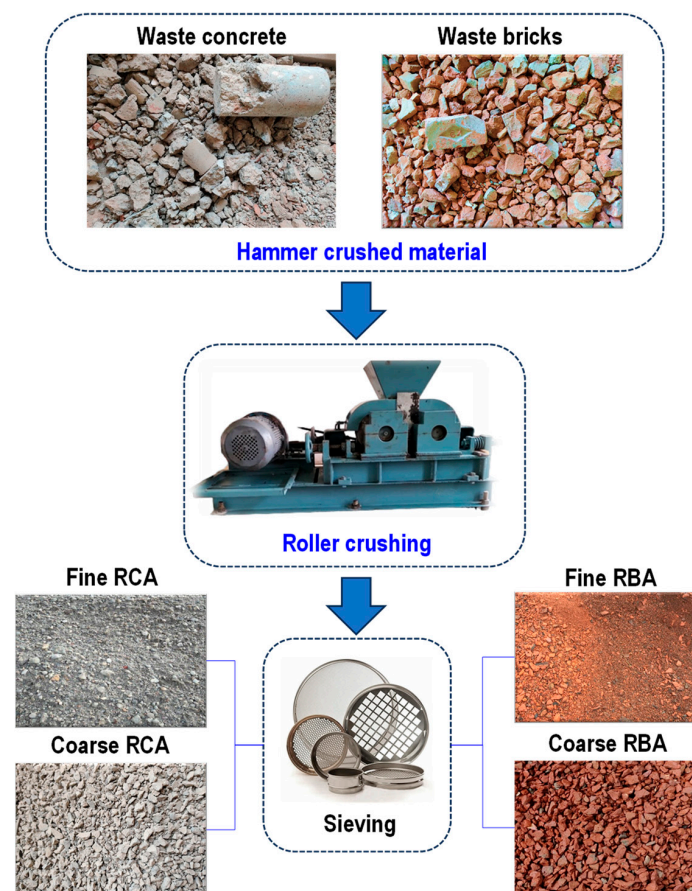


Figure 1. Production of recycled concrete and brick aggregates.

Table 1. Properties of aggregates.

Properties	Testing Standard	Aggregate Type					
		RCA		RBA		NA	
		Coarse	Fine	Coarse	Fine	Coarse	Fine
Bulk oven dry-specific gravity		2.21	2.05	1.74	1.58	2.71	2.59
Bulk SSD-specific gravity	ASTM C127 [58] and ASTM C128 [59]	2.49	2.29	2.04	1.85	2.85	2.75
Bulk Apparent-Specific Gravity		2.92	2.76	2.51	2.43	3.13	2.94
Water Absorption (%)		7.87	9.5	15.25	19.25	1.9	2.24
Bulk Density (kg/m ³)	ASTM C29 [60]	1321	1426.3	1290	1378.3	1532.6	1654.6
Crushing Value of Aggregate, ACV (%)	BS 812-110 [61]	22.4	-	38.57	-	14.2	-
Impact Value of Aggregate, AIV (%)	BS 812-112 [62]	18.1	-	31.46	-	12.78	-

A concrete admixture, namely Chemrite-SP-303, based on derivatives of carboxylic acid, was employed as a superplasticizer in this work to enhance the workability of RAC and also to improve its resistance to plastic and drying shrinkage. The density of this admixture at 25 °C was 1.06 ± 0.01 kg/L. To prepare all concrete mixes, ordinary Portland cement (OPC) of 42.5N class was used as binding material.

2.2. Concrete Mixes

In this research, a total of thirteen concrete mixes were made and used to prepare test specimens for compressive strength tests, pull-out tests, and flexure tests. Table 2 provides the details of these concrete mixes with respect to the type and content of fine and coarse aggregates used. The mix ratio of cement, fine aggregates, and coarse aggregates for all concrete mixes was kept the same at 1:2:3. For the designation of concrete mixes given in Table 2, F stands for fine aggregates and C stands for coarse aggregates. In brackets, the types of fine and coarse aggregates are given. For instance, the designation “F(RBA) + C(RBA)” shows a mix containing 100% fine RBAs and 100% coarse RBAs. In the designation of all concrete mixes in which coarse NAs along with coarse RCAs or RBAs are used, the percentage content of NAs and RAs is also provided. For instance, the designation “F(RBA) + C(75RBA + 25NA)” indicates a concrete mix made using 100% fine RBAs, 75% coarse RBAs, and 25% coarse NAs. Similarly, the designation “F(RCA) + C(50RCA + 50NA)” indicates a mix made using 100% fine RCAs, 50% coarse RCAs, and 50% coarse NAs. The details of the control mix are also provided in this table, which was prepared using 100% fine and coarse NAs.

Table 2. Concrete mixes.

Sr. No	Mix Designation	Fine Aggregates (%)			Coarse Aggregates (%)		
		RBAs	RCAs	NAs	RBAs	RCAs	NAs
1	F(RBA) + C(RBA)				100	-	-
2	F(RBA) + C(RCA)	100	-	-	-	100	-
3	F(RBA) + C(NA)				-	-	100
4	F(RCA) + C(RBA)				100	-	-
5	F(RCA) + C(RCA)	-	100	-	-	100	-
6	F(RCA) + C(NA)				-	-	100
7	F(RBA) + C(75RBA + 25NA)				75	-	25
8	F(RBA) + C(50RBA + 50NA)	100	-	-	50	-	50
9	F(RBA) + C(25RBA + 75NA)				25	-	75
10	F(RCA) + C(75RCA + 25NA)				-	75	25
11	F(RCA) + C(50RCA + 50NA)	-	100	-	-	50	50
12	F(RCA) + C(25RCA + 75NA)				-	25	75
13	CONT-F(NA) + C(NA)	-	-	100	-	-	100

2.3. Test Specimens

Tests to find strength in compression were carried out on specimens (cylinders) of diameter 100 mm and height 200 mm. In this study, direct pull-out tests were performed on a cubic ($200 \text{ mm} \times 200 \text{ mm} \times 200 \text{ mm}$) specimen. A deformed steel bar of 13 mm in diameter was embedded in the center of each pull-out test sample. The steel bars were prepared to ensure an embedded length of $5d_b$ [63,64] (d_b is the diameter of the steel bar) at the center of the specimen, as presented in Figure 2. To avoid bonding the steel bar with concrete at both ends (unbonded length), the steel bar was passed through the plastic pipes, as shown in Figure 2.

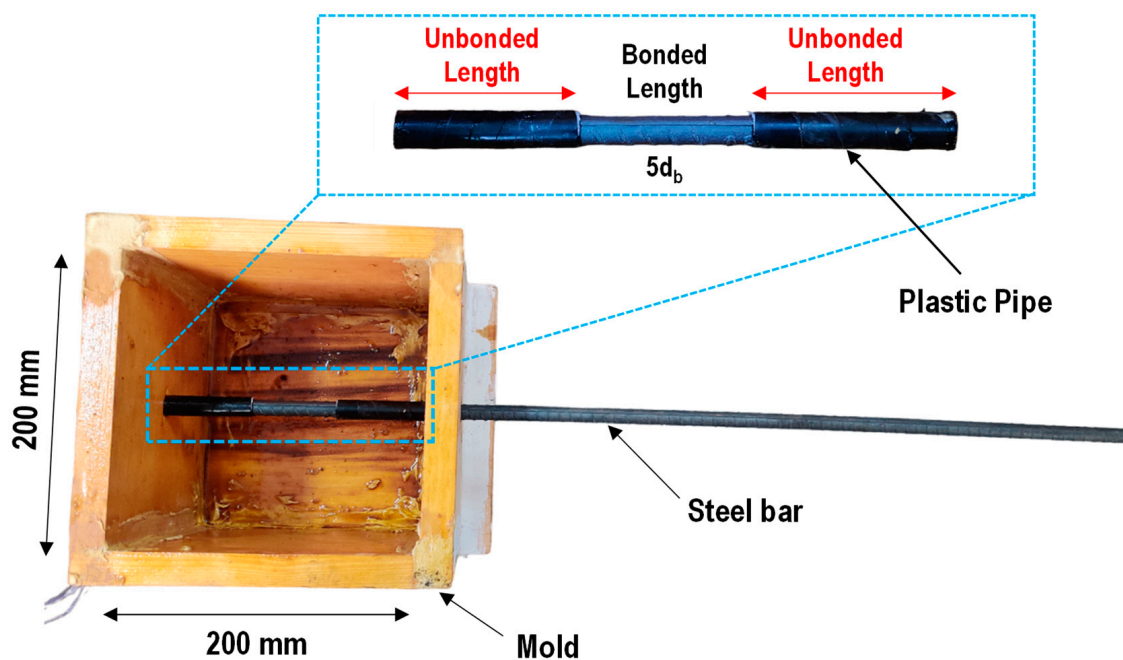


Figure 2. Sample preparation for the pull-out test.

The inner end of each plastic pipe was sealed with the help of silicon to avoid the penetration of cement slurry inside the pipe. For each concrete mix given in Table 1, two specimens were cast. To study the flexure response of all concrete mixes prepared in this study, RC beams of cross-section $100 \text{ mm} \times 200 \text{ mm}$ and length 1650 mm were prepared and tested under four-point bending. The testing span for each RC beam was kept at 1500 mm. Each RC beam was reinforced with 2 longitudinal bars of 10 mm diameter at the bottom, while 2 longitudinal steel rebars of 6 mm diameter were used as hanger bars. To avoid premature failure in shear, 2-legged shear reinforcement was provided using 6 mm diameter steel bars at 85 mm center to center. The shear reinforcement was provided up to a span/3 distance from both ends. The reinforcement detail of each RC beam is shown in Figure 3. In order to study the tensile strain development in the tension steel, strain gages were pasted on both bottom steel bars at the midspan section of each RC beam, as shown in Figure 4.

Based on the fact that the water absorption of RAs and Nas was different, as indicated in Table 1, both coarse RCAs and RBAs were used in the saturated surface dry (SSD) condition. For this purpose, the aggregates were dipped in water for 24 h and then placed in an open environment to dry their surfaces before their use in making concrete. For all concrete mixes, the w/c ratio (0.55) was kept constant. After 24 h of casting, all prepared test samples were placed in a controlled environment of 25°C and a relative humidity of 95% until the day of testing, which was carried out at 28 days of age.

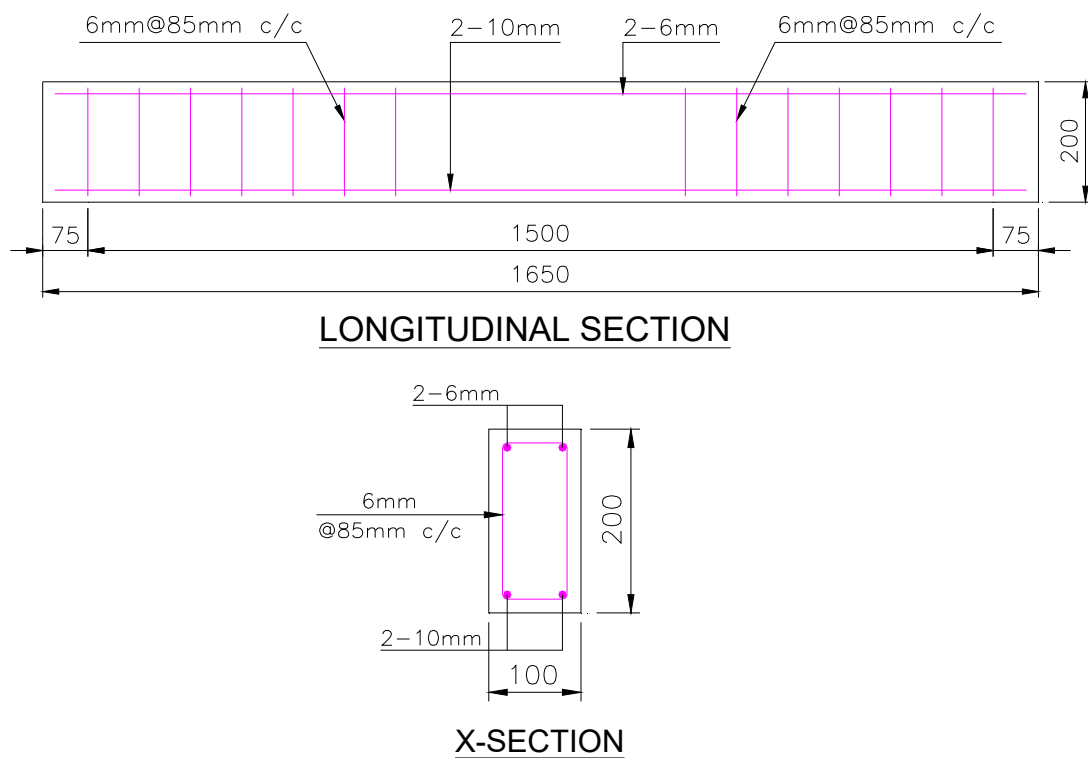


Figure 3. Reinforcement detail of RC beam.

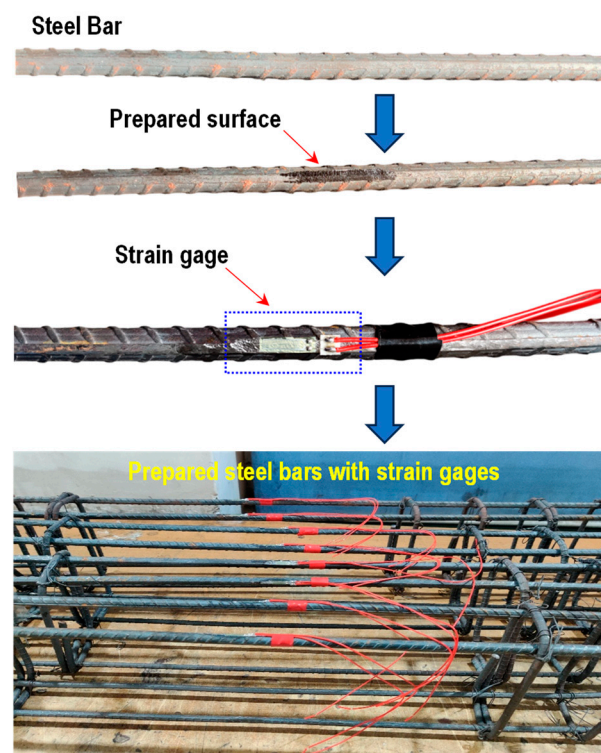


Figure 4. Preparation of steel bars for RC beams.

3. Test Methods

3.1. Density

The density of hardened concrete was measured in accordance with ASTM C642 [65]. Initially, concrete cylinders were placed in an oven for 24 h at a temperature of 100–110 °C,

and then they were placed at a temperature of 20–25 °C for cooling. After cooling, their dry mass (m) was measured. The density of concrete cylindrical samples was calculated using Equation (1):

$$\rho = \frac{m}{v} \quad (1)$$

where ρ = density of concrete (kg/m^3), m = mass of the specimen (kg), and v = volume of the concrete specimen (m^3).

3.2. Test for Compressive Strength

The tests were performed on cylindrical samples following the procedure given in ASTM C39 [66] on UTMs with a maximum 2000 kN capacity. The maximum load carried by each test specimen was noted, and the same was used to compute their compressive strength. Three samples were tested for each concrete mix given in Table 1, and the average value of their strength in compression has been reported in this paper.

3.3. Pullout Tests

These tests were performed using a UTM with a maximum loading capacity of 1000 kN, following the guidelines of ACI 440.3R-04 [67]. The testing setup used to perform this test is presented in Figure 5, where it is shown that a linear variable differential transducer (LVDT) was fixed at the top of the steel bar to measure its end slip during pulling out. A digital load cell was used to record the load value corresponding to the slip value. The loading rate for all pull-out tests was kept constant at 0.5 mm/min. During these tests, the slip and load data were automatically recorded using an automatic data acquisition system, and the same were used to investigate the bond stress vs. slip response of steel rebar embedded in various concretes in this study. For each concrete mix, two samples were tested for pull-out response.

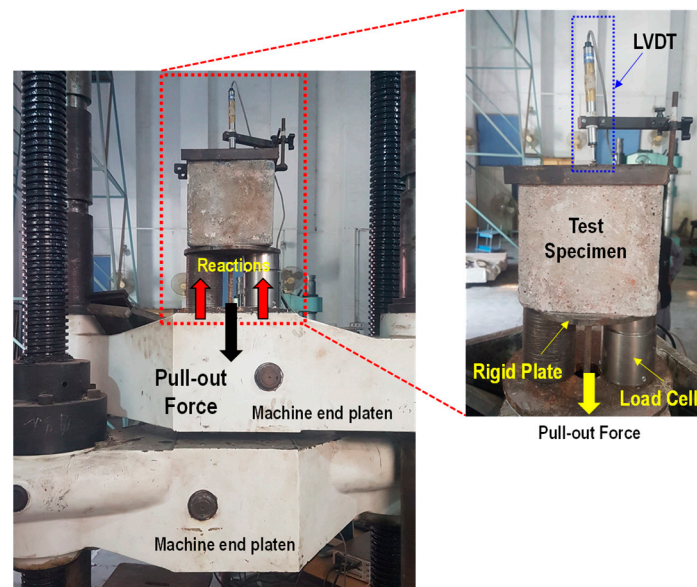


Figure 5. Test setup for the pull-out test.

3.4. Flexural Test

To examine the impact of fine and coarse RAs on the flexure behavior of the RC beam, displacement-controlled four-point flexure tests were performed at a loading rate of 1.0 mm/min using a 1000 kN universal testing machine. The testing setup used for these tests is shown in Figure 6, where it is shown that a rigid steel beam was used to divide and transfer the load at two locations (i.e., span/3 from each end). A digital load cell of 1000 kN capacity was used to record the load at each value of imposed displacement. The

values of imposed displacement, load from the load cell, and strain in tension steel bars from strain gages were recorded automatically using a data acquisition system. Further, for each test, the pattern of flexure cracks was visually observed and noted for the purpose of comparison among the different RC beams made in this study with respect to the different concrete compositions mentioned in Table 2. For each concrete composition, two RC beams were constructed and tested for their flexural response.

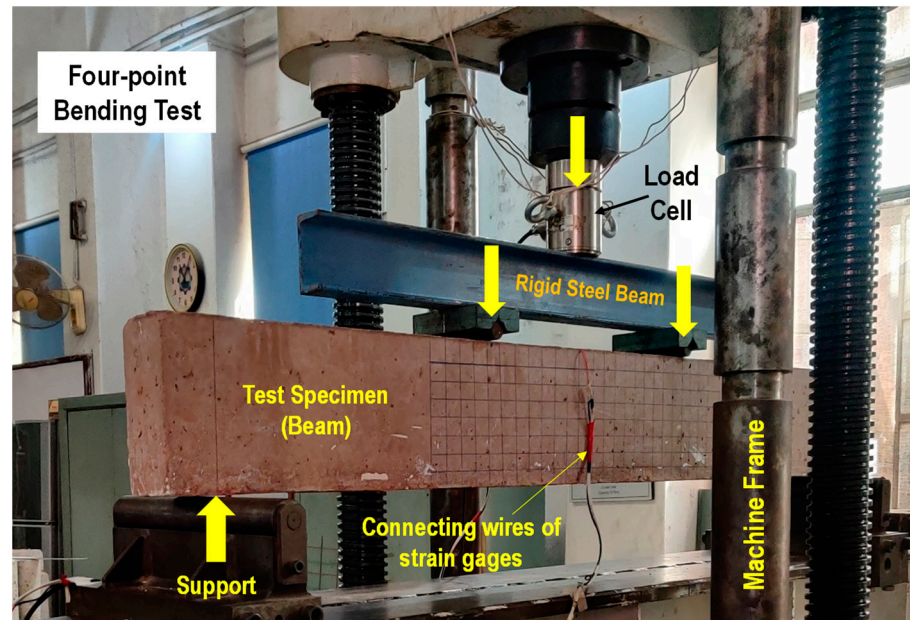


Figure 6. Test setup for the four-point bending test.

4. Results and Discussion

4.1. Density

The density of concrete prepared using all mixes given in Table 2 is presented in Figure 7, where it is noticed that the replacement of fine and coarse NAs with RAs caused a drop in the density of the resulting concrete. This is mainly attributed to the lower density of RBAs and RCAs compared to NAs given in Table 1. RAC containing both fine and coarse RBAs exhibited a density 23.6% lower than the control concrete; however, keeping the fine aggregates the same (i.e., RBAs) and replacing 100% coarse RBAs with RCAs resulted in an increase in density of 14.7%. Similarly, in comparison of F(RBA) + C(RBA) mix, keeping the fine aggregates the same (i.e., RBA) and gradually replacing 25%, 50%, 75%, and 100% coarse RBAs with coarse NAs resulted in an increase in concrete density of 3.5%, 11%, 14%, and 19%, respectively. However, their density remained less than that of control concrete. The results further showed that RAC containing both fine and coarse RCAs exhibited a density 11.4% lower than the control concrete; however, keeping the fine aggregates the same (i.e., RCAs) and replacing 100% coarse RCAs with RBAs resulted in a further decrease in density by 9.8% when compared to the density of the F(RCA) + C(RCA) mix. Similarly, in comparison to the F(RCA) + C(RCA) mix, keeping the fine aggregates the same (i.e., RCAs) and gradually replacing 25%, 50%, 75%, and 100% coarse RCAs with coarse NAs resulted in an increase in concrete density of 0.9%, 2.4%, 3.9%, and 6.9%, respectively. However, their density remained less than that of control concrete, as shown in Figure 7. Among the two RAs used in this study (i.e., RBAs and RCAs), the drop in density of hardened concrete was higher with RBAs, which was mainly because of their low bulk density, as given in Table 1.

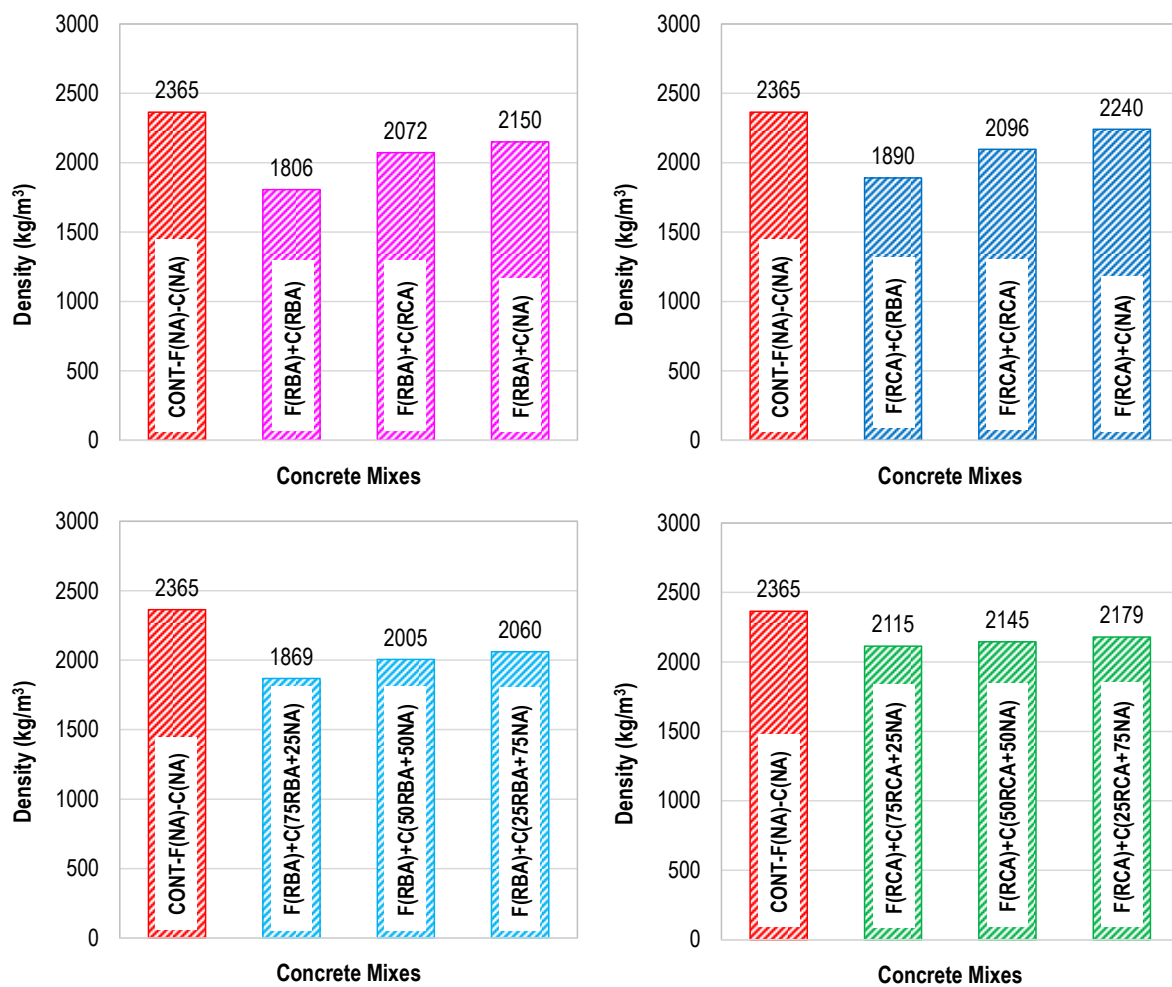


Figure 7. Concrete density (CONT = control mix, NA = natural aggregate, RBA = recycled brick aggregate, and RCA = recycled concrete aggregate).

4.2. Compressive Strength

The compressive strength tests on specimens prepared with the 13 various concrete mixes mentioned in Table 2 were conducted after 28 days of casting, and the results (average of three samples with a maximum variation of 7% in values) are presented in Figure 8. As indicated, the compressive strength exhibited by all RAC mixes satisfied the minimum requirement of strength for structural concrete given in ACI 318. Among all mixes, the maximum strength of 24.6 MPa was attained by the control mix containing 100% fine and coarse NA [F(NA) + C(NA)]. However, replacement of 100% fine NAs with fine RBAs [F(RBA) + C(NA)] in this mix resulted in a drop in compressive strength of 6.1%, while the drop in compressive strength was 8.9% when 100% fine NAs were replaced with fine RCAs [F(RCA) + C(NA)]. Since brick waste generally consists of aluminates and silicates, its pozzolanic characteristics [68] result in a significant drop in the compressive strength of concrete mix. Concrete mixes containing 100% fine and coarse RBAs attained 21.9% lower compressive strength compared to the control mix; however, the replacement of 100% coarse RBAs in this mix with coarse RCAs and coarse NAs increased the compressive strength by 2.6% and 20.3%, respectively. Similarly, concrete mix containing 100% fine and coarse RCAs (i.e., F(RCA) + C(RCA)) exhibited 20.7% lower compressive strength compared to the control mix (i.e., F(NA) + C(NA)); however, the replacement of 100% coarse RCAs in this mix with coarse RBAs decreased the strength by 4.1% while replacement of 100% coarse RCAs with coarse NAs increased the compressive strength by 14.9%. For concrete mixes with the same fine RAs, altering the replacement level of coarse NAs with

coarse RAs caused a gradual change in the compressive strength. Compared to a mix containing 100% fine RBAs and 100% coarse NAs [F(RBA) + C(NA)], the replacement of coarse NAs with coarse RBAs in the mix at rates of 25%, 50%, 75%, and 100% decreased the compressive strength by 5.2%, 9.5%, 12.5%, and 16.8%, respectively. Similarly, in comparison of concrete mix containing 100% fine RCAs and 100% coarse NAs [F(RCA) + C(NA)], replacement of coarse NAs with coarse RCAs in the mix at the rate of 25%, 50%, 75%, and 100% decreased the compressive strength by 4.0%, 8.5%, 10.3%, and 12.9%, respectively. The results of compressive strength clearly revealed that although fine and coarse RAs imparted a negative effect on the concrete strength, in the presence of fine RBAs in the mix, the drop in compressive strength of RAC, compared to the control mix, was lower than that of other RAC mixes. This may be attributed to the cementing ability of fine RBAs, as highlighted by the previous research studies. On the contrary, the detrimental effect on the concrete strength was higher with coarse RBAs compared to coarse RCAs.

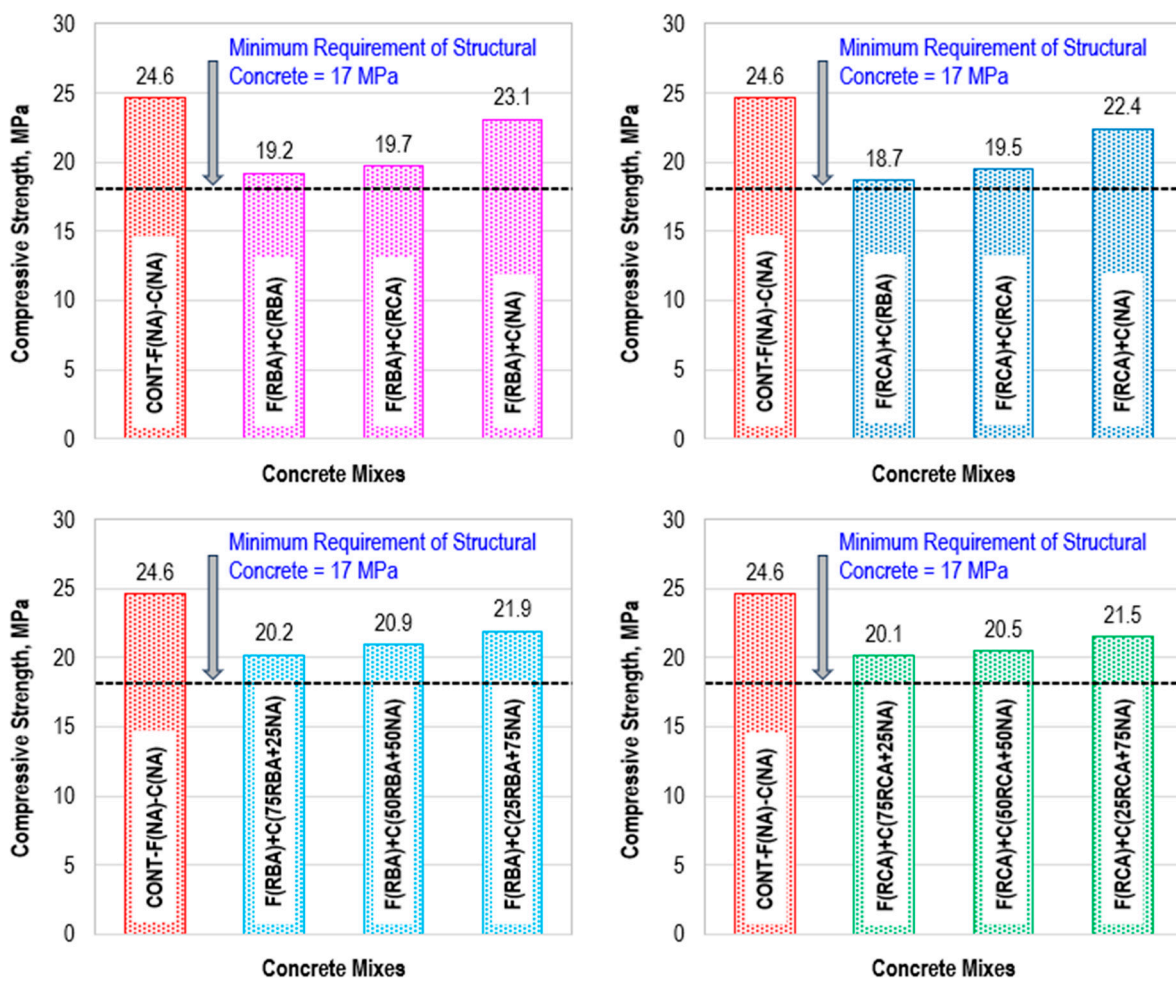


Figure 8. Compressive strength results (Minimum compressive strength requirement of structural concrete is 17 MPa [46]).

4.3. Bond Strength

The impact of different RAs on the bond performance of steel rebar embedded in RAC was evaluated by pullout tests. The average bond strength was determined using the following equation, where F is the maximum experimental force obtained in pull out tests, d_b is the diameter of the embedded steel bar, and l_b is the bonded length (i.e., taken as equal to $5 d_b$ in this study):

$$\tau = \frac{F}{\pi d_b l_b} \tag{2}$$

The data obtained from pull-out tests for each concrete mix were analyzed in terms of bond stress–slip response, as presented in Figures 9 and 10 (average of two samples with a maximum variation of 9% in values). Since the compressive strength of concrete mix significantly affects the maximum bond strength, the peak bond strength exhibited by each concrete mix was normalized by its compressive strength, as indicated in Equation (3):

$$\tau_n = \frac{\tau_{max}}{\sqrt{f'_c}} \tag{3}$$

where τ_n is the normalized bond strength, τ_{max} is the maximum bond stress, and f'_c is the compressive strength of the concrete. The maximum and normalized bond strength values of all concrete mixes are presented in Figures 11 and 12, respectively.

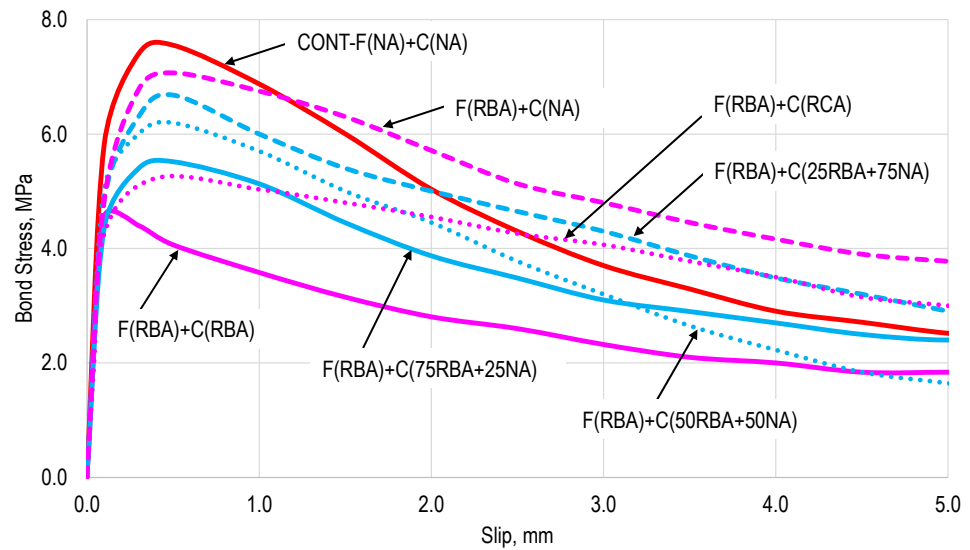


Figure 9. Bond stress–slip response (mixes containing fine RBAs).

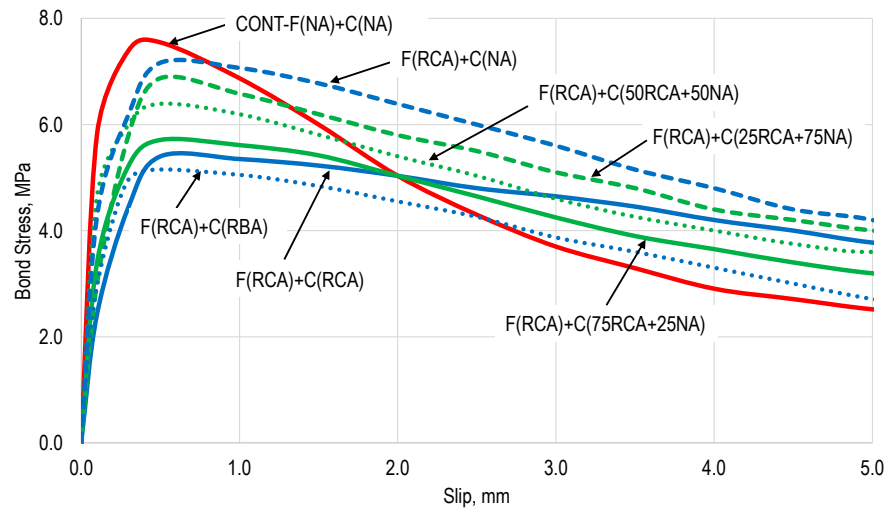


Figure 10. Bond stress–slip response (mixes containing fine RCAs).

The bond stress vs. slip response of concrete mixes containing 100% fine RBAs is presented in Figure 9, along with the same response of the control concrete mix. Among these mixes, the lowest response was exhibited by the mix containing 100% coarse RBAs (i.e., F(RBA) + C(RBA)). However, an improvement in the overall response was observed when coarse RBAs were partially or fully replaced with coarse NAs. It was noticed that the post-peak bond behavior of concrete mix containing 100% fine RBAs and 100% coarse NAs was even better than the control concrete mix (i.e., F(NA) + C(NA)). Due to the presence

of weak RBAs, the bearing strength of RAC in contact with the ribs of a deformed steel bar is significantly reduced, causing early development and quick propagation of splitting cracks in the relatively weak concrete matrix surrounding the steel bar. Consequently, a detrimental effect on bond strength and a sharp degradation of the post-peak bond stress–slip response in RAC were observed. However, the replacement of weak coarse RBAs with relatively stronger coarse NAs in the concrete mix gradually improved its overall bond stress–slip response. The results presented in Figure 9 revealed that the replacement of 100% coarse RBAs with RCAs improved the overall response of concrete when compared to a concrete mix containing 100% coarse RBAs. The positive impact of coarse RCAs on the residual bond strength at a larger slip value was obvious from the results of this study. The slip of deformed steel rebar corresponding to peak bond strength was almost similar for all concrete mixes except for the mix containing 100% fine and coarse RBAs [F(RBA) + C(RBA)], where it was significantly less.

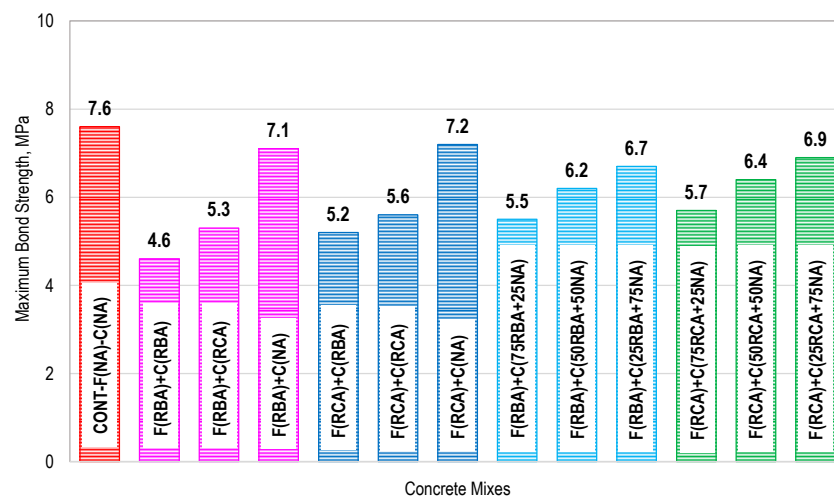


Figure 11. Maximum bond strength.

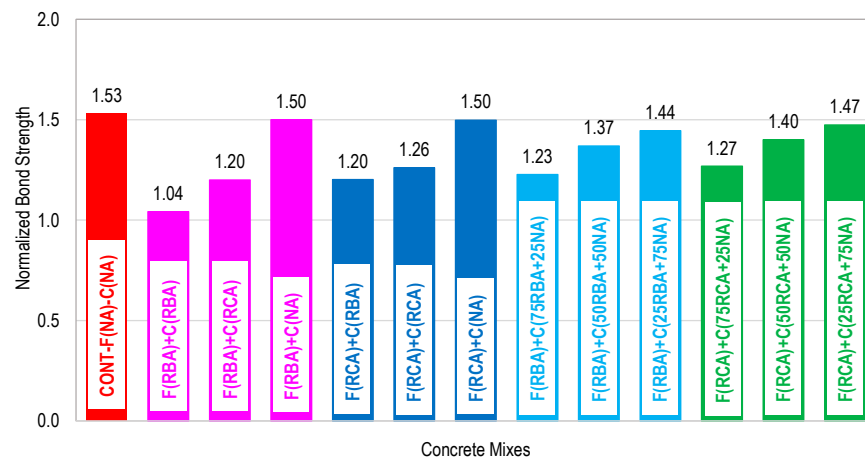


Figure 12. Normalized bond strength.

The bond stress–slip response of concrete mixes containing 100% fine RCAs is presented in Figure 10 along with the response of the control concrete mix. The peak bond strength exhibited by all RAC mixes was less than the bond strength of the control mix; however, the slip value at peak bond strength for RAC mixes containing fine and coarse RCAs was higher than that of the control mix. The results clearly indicated that the replacement of coarse RCAs with coarse NAs improved the overall bond performance of steel rebar in concrete. At slip greater than 2 mm, the residual bond strength of RAC mixes containing 100% coarse RCAs or coarse RCAs and NAs was observed to be higher than

the control mix. This may be attributed to the fact that the crushing of waste concrete to produce RAs generally results in particles with higher angularity. This property of RCAs plays a positive role in enhancing frictional resistance between steel bars and concrete at larger slip values, resulting in improved residual bond strength.

The maximum bond strength exhibited by each concrete mix presented in Table 2 is presented in Figure 11, where it is noticed that the bond strength attained by the control mix was higher compared to RAC mixes containing RBAs or RCAs. By replacing fine NAs with fine RBAs in the control mix, the bond strength dropped by 7%, while the reduction in bond strength was 6% when fine NAs were replaced with fine RCAs. Concrete mix containing 100% fine and coarse RBAs exhibited bond strength 40% less than the control mix; however, in the same mix, replacement of 100% coarse RBAs with 100% RCAs and NAs enhanced the bond strength by 15% and 54%, respectively. Similarly, the RAC mix containing 100% fine RCAs and 100% coarse RBAs exhibited a bond strength 31% less than the control mix; however, in the same mix, the replacement of 100% coarse RBAs with 100% RCAs and NAs enhanced the bond strength by 7% and 38%, respectively. Compared to RAC mix containing 100% fine and coarse RBAs (i.e., F(RBA) + C(RBA)), the replacement of coarse RBAs with 25%, 50%, and 75% coarse NAs improved the bond strength by 19%, 34%, and 45%, respectively. Similarly, compared to the RAC mix containing 100% fine and coarse RCAs (i.e., F(RCA)+C(RCA)), the replacement of coarse RCAs with 25%, 50%, and 75% coarse NAs enhanced the bond strength by 2%, 14%, and 23%, respectively.

Prediction of Bond Strength

To predict bond strength between concrete and steel rebars, existing models proposed by past researchers for NAC, described below, have been employed in this study. Similarly, the model proposed by Hoque et al. [45] for brick aggregate concrete has also been used.

Hoque et al. [45] studied bond behavior between brick aggregate concrete (BAC) and reinforcing rebars. For this purpose, they tested cylindrical as well as cubic specimens having design strengths of 20, 25, and 30 MPa. The several varying test parameters were also studied to assess their influence on the bond strength, which included bond length, bar diameter, concrete confinement, concrete compressive strength, and specimen shape. Finally, they proposed Equation (4) based on experimental results for the estimation of bond strength between BAC and rebar. In Equation (5), f'_c = concrete compressive strength, c = concrete cover, and d_b = diameter of the embedded bar.

$$\tau = 0.525\sqrt{f'_c}\left(\frac{c}{d_b}\right)^{0.42} \quad (4)$$

ACI 318-19:

To predict bond strength between natural stone aggregate concrete and rebar, the ACI 318-19 [46] proposed the following equation:

$$\tau = \frac{A_b f_y}{\pi d_b l_d} \quad (5)$$

where A_b = area of the rebar, f_y = yield strength of steel, d_b = diameter of rebar, and l_d = development length of the specified bar that can be calculated using the following equation:

$$l_d = \left(\frac{f_y \psi_t \psi_e \lambda}{2.1 \sqrt{f'_c}}\right) d_b \quad (6)$$

The details of all parameters used in this equation may be found in reference [46]. In this study, steel bars of diameter 12.7 mm were used. The yield strength of the rebar was 415 MPa, and ψ_t and ψ_e were assumed to be one based on the specified conditions of the experiment.

Australian standard AS 3600:

According to Australian standard AS 3600 [69], following Equation (7) can be employed to calculate the bond strength between the natural stone aggregate concrete and the rebar, where f'_c = concrete compressive strength, c = concrete cover, and d_b = diameter of the rebar.

$$\tau = 0.265\sqrt{f'_c}\left(\frac{c}{d_b} + 0.5\right) \tag{7}$$

CEB-FIP model:

According to the CEB-FIP model [70], bond strength depends upon the type of failure and bond condition, as given in Table 3. The equations proposed by the CEB-FIP model for the measuring bond strength of reinforcing bars embedded in natural stone aggregate concrete are also proven in this table. For all samples tested in this study, pull-out failure mode was observed as a dominant failure type, and a good condition of the bond was assumed to calculate bond strength, and accordingly, model (e) was used to calculate bond strength.

Table 3. The CEB-FIP empirical models for bond strength.

Failure Type	Bond Condition		Bond Strength (MPa)	Equation No.
Splitting Failure	Good	Unconfined	$7.0 \left(\frac{f_{ck}}{20}\right)^{0.25}$	(8)
		Confined	$8.0 \left(\frac{f_{ck}}{20}\right)^{0.25}$	(9)
	Other	Unconfined	$5.0 \left(\frac{f_{ck}}{20}\right)^{0.25}$	(10)
		Confined	$5.5 \left(\frac{f_{ck}}{20}\right)^{0.25}$	(11)
Pull-out failure	Good	$2.5 \sqrt{f_{ck}}$	(12)	
	Other	$1.25 \sqrt{f_{ck}}$	(13)	

A comparison of experimentally obtained bond strength and predicted bond strength using existing models is presented in Figure 13. This comparison revealed that the bond strength predictions of the Hoque et al. [45] model are in good agreement with the experimental data on the bond strength of RAC mixes containing 100% fine RBAs and varying percentages of coarse RBAs in place of coarse NAs (Figure 13a) and are in fair agreement with the experimental bond strength of RAC mixes containing 100% fine RCAs and varying percentages of coarse RCAs in place of coarse NAs (Figure 13b). However, the bond strength determined using the model proposed by ACI 318-19 was almost half of the experimental values of RAC mixes. On the contrary, compared to experimental results, the AS 3600 and CEB-FIP models overestimated the bond strength for RAC mixes containing RBAs or RCAs, as shown in Figure 13.

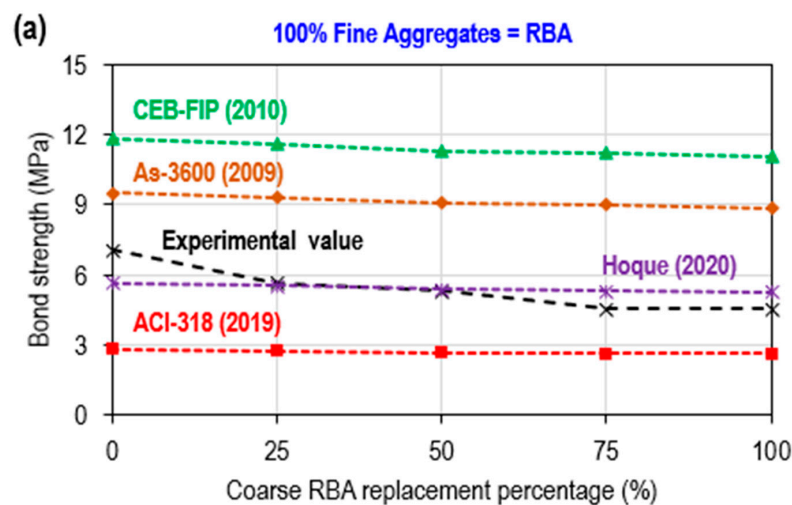


Figure 13. Cont.

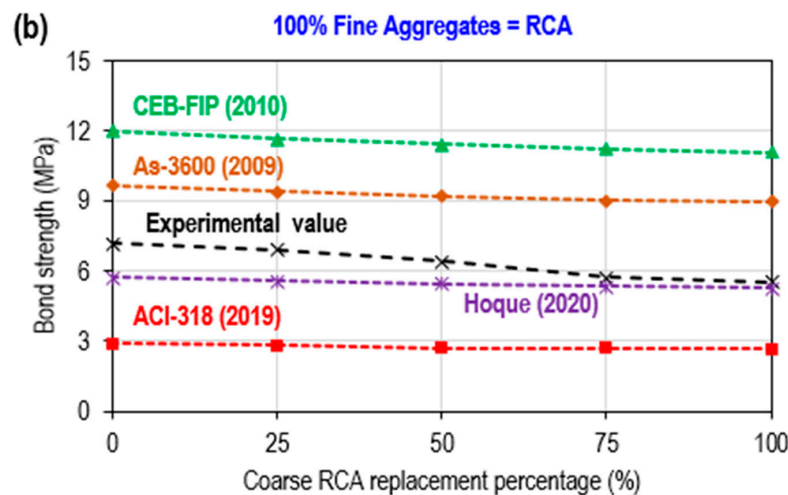


Figure 13. Comparison of experimental and predicted bond strength: (a) Coarse RBA replacement percentage, (b) Coarse RCA replacement percentage.

4.4. Flexural Test Results

4.4.1. Load–Deflection Response

Load–deflection behavior curves in the bending of RC beams constructed using RAC mixes given in Table 1 are presented in Figure 14. For comparison, the same behavior of the RC beam made using the NAC (control beam) has also been presented in the same graph. In general, the overall trend in load–deflection response of RC beams made using RAC and NAC was almost the same. For the RC beam containing 100% fine RBAs and coarse RBAs (partially or fully), the load carrying capacity was on the lower side compared to the control beam; however, at each deflection value, it was improved by replacing coarse RBAs with coarse NAs or RCAs (Figure 14a,c). It is obvious from the results that the load vs. deflection behavior of RC beams with RCAs was better than the ones containing RBAs. The results presented in Figure 14d revealed that RC beams containing 100% fine RCAs and coarse RCAs at varying contents exhibited a response similar to the control beam.

4.4.2. Cracking and Yielding Moments

The bending moment capacity of all RC beams corresponding to experimental loads at first cracking (i.e., cracking moment) and yielding of steel bars (i.e., yielding moment) were determined and then compared with theoretical values of cracking and yielding bending moments computed as per the guidelines of ACI-318 [46] by employing Equations (14) and (15). In these equations, M_{cr} = cracking moment, f_r = modulus of rupture calculated as $0.62\sqrt{f'_c}$, I_g = gross moment of inertia, y_t = distance from the centroid to the extreme fiber in tension, M_{yiel} = yield moment capacity, A_s = area of bottom longitudinal reinforcement, f_y = yielding stress of steel, d = distance from the extreme compression fiber to the center of bottom steel bar, and a = depth of rectangular stress block from the top.

$$M_{cr} = \frac{f_r I_g}{y_t} \quad (14)$$

$$M_{yiel} = A_s f_y \left(d - \frac{a}{2} \right) \quad (15)$$

The comparison of theoretical and experimental values of cracking and yielding moment capacity of RC beams prepared with concrete mixes presented in Table 1 is graphically presented in Figures 15 and 16, respectively. For all beams, the experimental value of the cracking moment was higher than the theoretical value. RC beams prepared using mixes containing 100% fine RAs (RBAs or RCAs) and 100% coarse NAs exhibited a cracking moment similar to that of the control RC beam. Since the theoretical prediction of M_{cr} mainly depends upon the modulus of rupture of the concrete matrix (calculated

as $0.62\sqrt{f'_c}$, the variation in M_{cr} due to aggregate type and its content followed a trend similar to compressive strength.

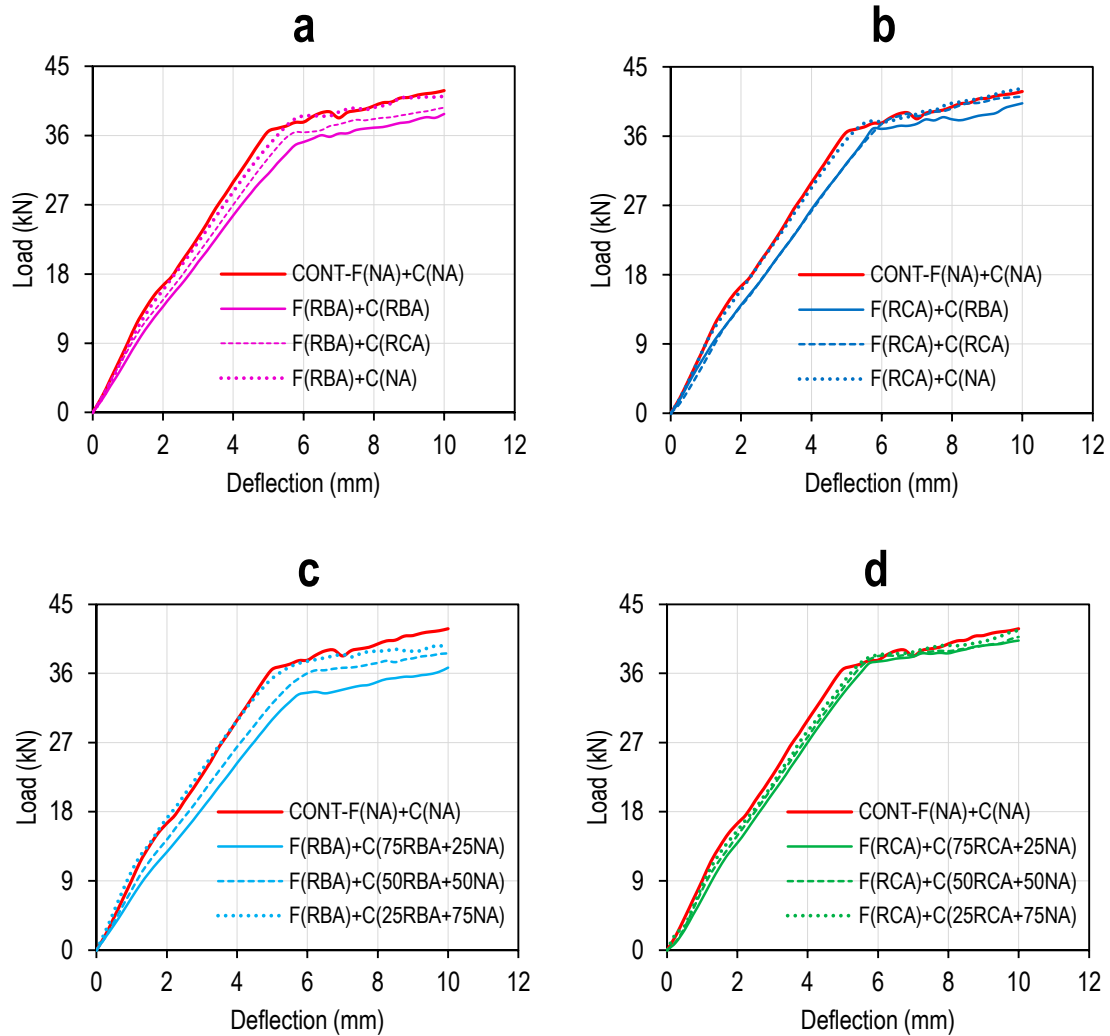


Figure 14. Load vs. deflection responses of RC beams: (a) Fine aggregates (RBA), (b) Fine aggregates (RCA), (c) Fine aggregates (RBA) and coarse aggregates (RBA and NA), (d) Fine aggregates (RCA) and coarse aggregates (RCA and NA).

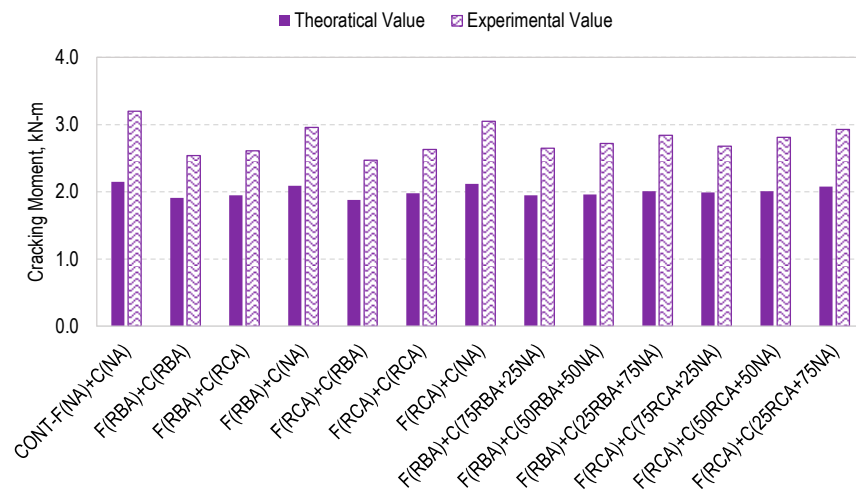


Figure 15. Cracking moment.

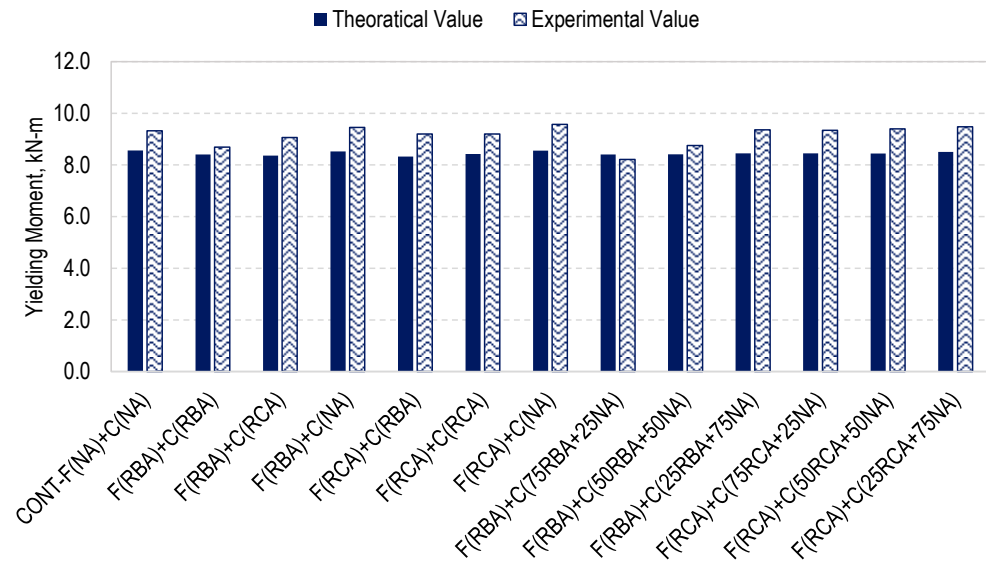


Figure 16. Yielding moment.

Variation in the strain in tension steel of RC beams measured using strain gages pasted at their midspan is shown in Figure 17. The trend of strain development or evolution in tension steel bars was found to depend on the type of fine and coarse aggregates used in the concrete mixes. Since in the case of reinforced concrete, the composite action between steel bars and concrete directly influences the transfer of stress to the steel bars and ultimately strain level, the pattern of changes in the tension steel strain was similar to the one observed for bond stress development with respect to the type and content of aggregates in concrete.

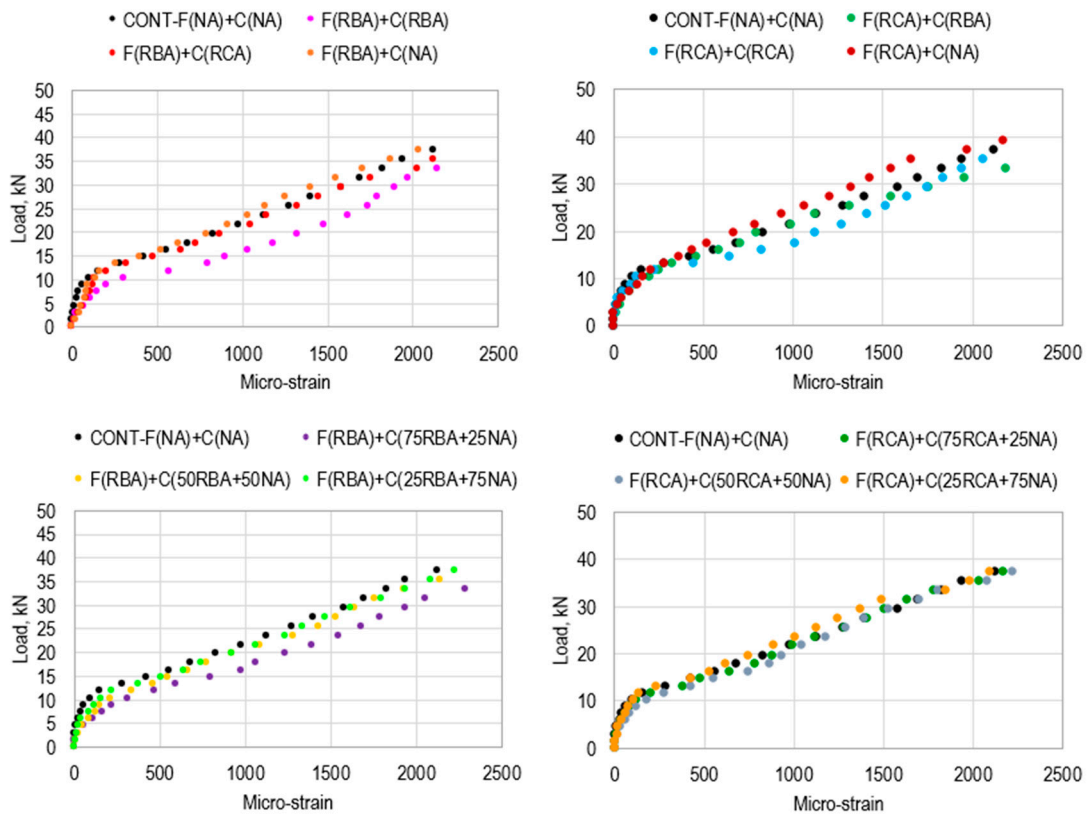


Figure 17. Strain in steel bars.

Moreover, the deflections at cracking (δ_{cr}) and yielding (δ_{yield}) were also measured, and the corresponding stiffness of the beams, k_{cr} and k_{yield} , respectively, were also calculated using Equation (16), where k is the stiffness of the beam at cracking or yielding, F is the load for cracking or yielding, and δ is the corresponding deflection at cracking and yielding points. The cracking and yielding stiffness were defined, as illustrated in Figure 18.

$$k = \frac{F}{\delta} \tag{16}$$

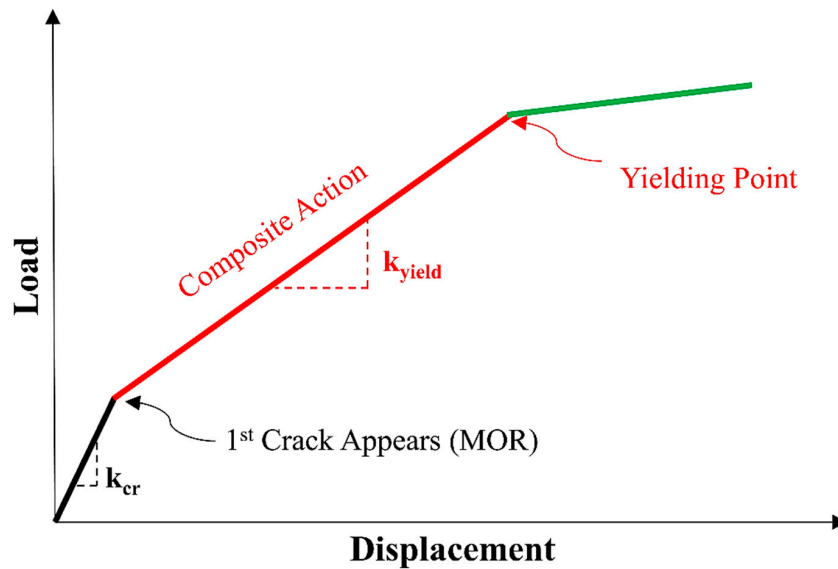


Figure 18. Definitions of cracking and yield stiffness.

Figure 19 illustrates the stiffness of the concrete with different replacement levels of coarse RAs (RBAs or RCAs) by NAs. The increase in the cracking stiffness of concrete prepared with the replacement of coarse NAs by 25% of RBAs was observed. However, with the increase in the content of coarse RBAs, a further decrease in cracking stiffness was observed. While, with the replacement of 100% coarse NAs with coarse RCAs, similar cracking stiffness was obtained for the specimens prepared with 100% NAs (control). However, at the yielding of the steel, similar stiffness was obtained for both types of coarse RAs, and the results obtained were close to those of the control specimens.

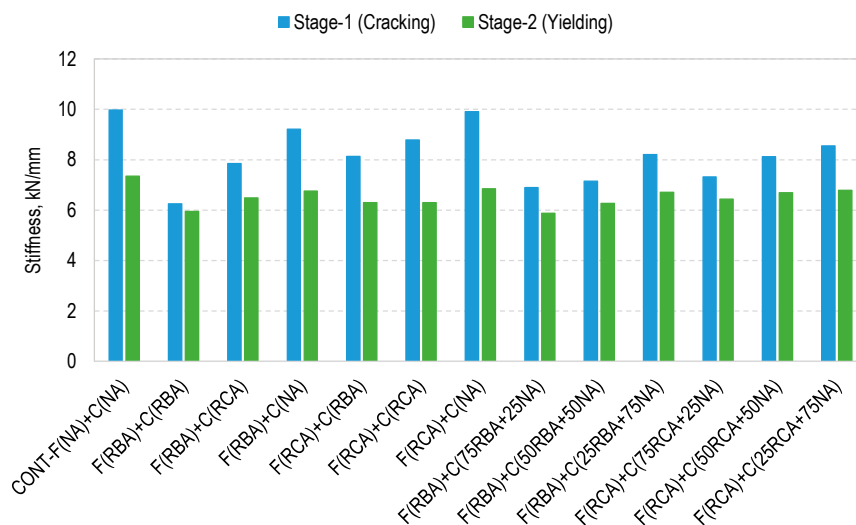


Figure 19. Stiffness before and after concrete cracking.

4.4.3. Cracking Patterns of RC Beams

The cracking pattern of each RC beam tested in this study is shown in Figure 20, while the crack spacing in each beam is shown in Figure 21. It was observed that cracks in the beams containing fine RBAs and either of the coarse aggregates exhibit more damage as compared to the other specimens, with the applied load approaching the yielding point.

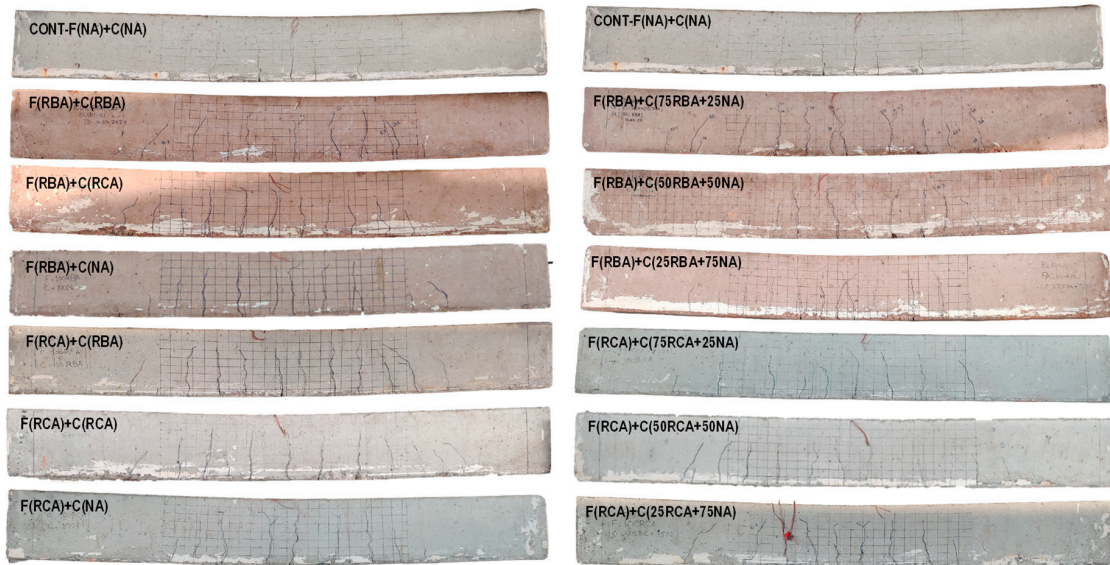


Figure 20. Cracking behavior of RC beams prepared with 100% RAs and 100% NAs.

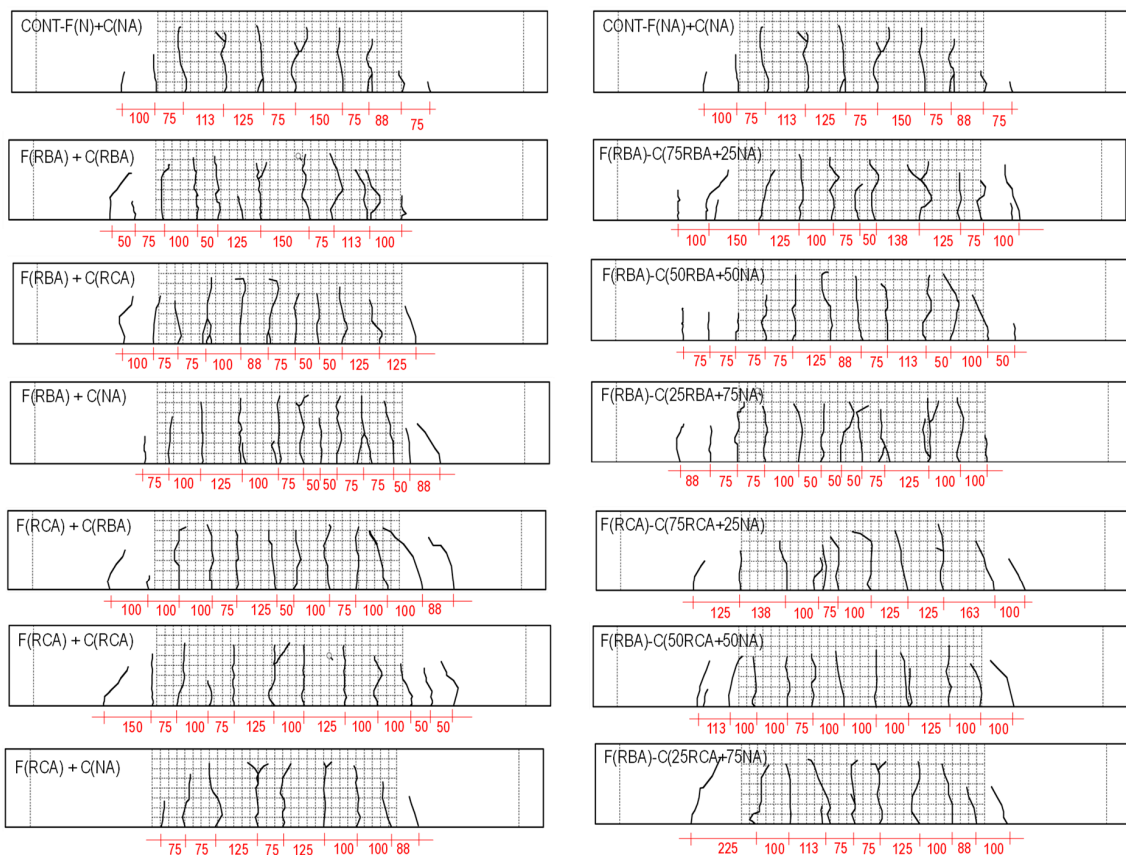


Figure 21. Crack spacing in all tested beams (in mm).

As a minimum area of reinforcement was provided in the beam, making them tension-controlled sections, initially, the flexural cracks originated from the center of the beam, and with the increase in load, cracks propagated towards the compression face. As the load was further increased, a few inclined flexure-shear cracks were formed, but no obvious cracks appeared in the vicinity of the shear zone. Finally, the flexural crack in the central region of the span expanded, and the beams failed because of the crushing of concrete in the compression zone. It was also observed that in the presence of recycled fine and coarse aggregates, the propagation of the cracks was quick as compared to the one that appeared in the specimens containing coarse NAs. Additionally, it was observed that the opening of the cracks in beams with recycled aggregates was higher compared to the control specimen because of their lower tensile strength and bond stress, as evaluated in the current research study, which was found to be consistent with the findings of past research [71,72].

5. Conclusions

The current research deals with the experimental evaluation of the bond and flexure behavior of reinforced recycled aggregate concrete prepared using RBAs and RCAs. The following conclusions can be drawn from the findings of this study:

- (1) The reduction in both compressive and bond strengths was observed with the increase in the content of coarse RAs in the mix composition. However, with a 50% replacement of NAs by RAs, the decrease in properties was insignificant. This highlights the potential of incorporating recycled materials into concrete mixes as a viable option for achieving satisfactory strength levels.
- (2) Among all tested specimens, the experimentally measured bond strengths exceeded the design values predicted using the empirical model proposed by ACI 318, indicating favorable bonding performance. Notably, while comparing specimens containing coarse RCAs to those prepared with coarse RBAs with the addition of any fine aggregate (RCA or RBA), a slightly higher bond strength was observed in the former.
- (3) The cracking and yielding stiffness of the beams show improvement for the specimens prepared with a higher content of coarse NAs. These findings highlight the influence of NAs on the stiffness characteristics of the beams, indicating that increasing the quantity of NAs can enhance the structural performance and load-bearing capacity of the concrete elements. However, the specimen containing 50% recycled coarse aggregates also showed comparable performance to the controlled specimen.
- (4) In the case of beams containing recycled coarse aggregates, an expanded pattern with a greater number of cracks was observed. On the other hand, beams with natural coarse aggregate and controlled specimens exhibited a squeezed pattern with fewer cracks. This disparity in crack patterns suggests that the use of recycled coarse aggregates can lead to increased cracking and a more dispersed distribution of cracks compared to beams with natural coarse aggregate. However, with the partial replacement of NAs by RAs, less damage was observed for the specimens in the presence of a higher content of NAs.

This study finally concludes that the flexural response of RC beams containing 100% fine recycled brick aggregates or fine recycled concrete aggregate is similar to the control RC beam; however, it is inferior to the control RC beam when natural coarse aggregates are fully replaced with coarse recycled brick aggregates. To maximize the use of coarse recycled aggregates in RC beams without compromising the strength, a hybrid form of recycled concrete and brick aggregates (75:25) has been found to be a good option.

This study mainly focused on the behavior of RC beams made using concrete containing RCAs and RBAs. The authors recommend carrying out future research studies on the behavior of RC columns constructed using similar concrete mixes. Further, experimental investigation to study the impact of suitable treatment methods on the properties of RBAs for their structural applications is also recommended to be carried out in future research.

Author Contributions: Conceptualization, R.H. and S.A.; Formal analysis, S.M.S.K. and M.J.M.; Funding acquisition, A.B., S.A., M.S.K., S.S., S.M.S.K. and M.J.M.; Investigation, R.H., S.A. and M.S.K.; Methodology, A.B., R.H., S.A., M.S.K. and S.S.; Project administration, R.H. and S.A.; Resources, A.B., R.H., S.A., S.M.S.K. and M.J.M.; Supervision, R.H.; Writing—original draft, A.B., R.H., S.A. and S.M.S.K.; Writing—review and editing, S.M.S.K. and M.J.M. All authors have read and agreed to the published version of the manuscript.

Funding: Higher Education Commission (HEC) of Pakistan under HEC-NRPU Project No. 9764.

Institutional Review Board Statement: Not applicable.

Informed Consent Statement: Not applicable.

Data Availability Statement: The original contributions presented in the study are included in the article, further inquiries can be directed to the corresponding author.

Acknowledgments: The authors would like to acknowledge the financial support of the Higher Education Commission (HEC) of Pakistan and the Civil Engineering Department, University of Engineering and Technology, Lahore, Pakistan.

Conflicts of Interest: The authors declare no conflicts of interest.

References

1. Aitkin, P.-C. Cements of yesterday and today: Concrete of tomorrow. *Cem. Concr. Res.* **2000**, *30*, 1349–1359.
2. Dalkılıç, N.; Nabikoğlu, A. Traditional manufacturing of clay brick used in the historical buildings of Diyarbakir (Turkey). *Front. Arch. Res.* **2017**, *6*, 346–359. [\[CrossRef\]](#)
3. Global Cement and Concrete Association (GCCA). *Global Cement and Concrete Industry Announces Roadmap to Achieve Ground-Breaking 'Net Zero' CO₂ Emissions by 2050*; Global Cement and Concrete Association (GCCA): London, UK, 2021.
4. Moujoud, Z.; Harrati, A.; Manni, A.; Naim, A.; El Bouari, A.; Tanane, O. Study of fired clay bricks with coconut shell waste as a renewable pore-forming agent: Technological, mechanical, and thermal properties. *J. Build. Eng.* **2023**, *68*, 106107. [\[CrossRef\]](#)
5. Weyant, C.; Kumar, S.; Maithel, S.; Thompson, R.; Baum, E.; Floess, E.; Bond, T. *Brick Kiln Measurement Guidelines: Emissions and Energy Performance*; Climate and Clean Air Coalition: Paris, France, 2016.
6. Anike, E.E.; Saidani, M.; Ganjian, E.; Tyrer, M.; Olubanwo, A.O. Evaluation of conventional and equivalent mortar volume mix design methods for recycled aggregate concrete. *Mater. Struct.* **2020**, *53*, 22. [\[CrossRef\]](#)
7. Gyawali, T.R. Re-use of concrete/brick debris emerged from big earthquake in recycled concrete with zero residues. *Clean. Waste Syst.* **2022**, *2*, 100007. [\[CrossRef\]](#)
8. Mountains of Debris' Rise in Türkiye's Quake-Hit Regions. Bianet—Bagimsiz Iletisim Agi. Available online: <https://www.bianet.org/english/environment/274692-mountains-of-debris-rise-in-turkiye-s-quake-hit-regions> (accessed on 1 August 2023).
9. Ahmad, M.; Hameed, R.; Shahzad, S.; Sohail, M.G. *Performance Evaluation of Loadbearing Compressed Fully Recycled Aggregate Concrete Bricks*; Elsevier: Amsterdam, The Netherlands, 2023; pp. 1235–1249.
10. Farooq, M.U.; Hameed, R.; Tahir, M.; Sohail, M.G.; Shahzad, S. Mechanical and durability performance of 100% recycled aggregate concrete pavers made by compression casting. *J. Build. Eng.* **2023**, *73*, 106729. [\[CrossRef\]](#)
11. Hameed, R.; Imran, M.; Hassan, M.I.; Arshad, E. Mechanical performance of 100% recycled aggregate concrete (RAC) bricks. *Rev. Constr.* **2023**, *22*, 203–222. [\[CrossRef\]](#)
12. Anike, E.E.; Saidani, M.; Ganjian, E.; Tyrer, M.; Olubanwo, A.O. The potency of recycled aggregate in new concrete: A review. *Constr. Innov.* **2019**, *19*, 594–613. [\[CrossRef\]](#)
13. Ghalehnovi, M.; Roshan, N.; Hakak, E.; Shamsabadi, E.A.; De Brito, J. Effect of red mud (bauxite residue) as cement re-placement on the properties of self-compacting concrete incorporating various fillers. *J. Clean. Prod.* **2019**, *240*, 118213. [\[CrossRef\]](#)
14. Tejas, S.; Pasla, D. Assessment of mechanical and durability properties of composite cement-based recycled aggregate concrete. *Constr. Build. Mater.* **2023**, *387*, 131620. [\[CrossRef\]](#)
15. Russo, N.; Lollini, F. Effect of carbonated recycled coarse aggregates on the mechanical and durability properties of concrete. *J. Build. Eng.* **2022**, *51*, 104290. [\[CrossRef\]](#)
16. Martínez-García, R.; de Rojas, M.S.; Jagadesh, P.; López-Gayarre, F.; Morán-Del-Pozo, J.M.; Juan-Valdes, A. Effect of pores on the mechanical and durability properties on high strength recycled fine aggregate mortar. *Case Stud. Constr. Mater.* **2022**, *16*, e01050. [\[CrossRef\]](#)
17. Reddy, R.S.R.; Sagar, B.A. Experimental study on mechanical and durability properties of recycled aggregate based geo-polymer concrete. *Mater. Today: Proc.* **2022**, *52*, 649–654. [\[CrossRef\]](#)
18. Hameed, R.; Tahir, M.; Shahzad, S.; Kazmi, S.M.S.; Munir, M.J. Impact of Compression Casting Technique on the Mechanical Properties of 100% Recycled Aggregate Concrete. *Sustainability* **2023**, *15*, 8153. [\[CrossRef\]](#)
19. Adessina, A.; Ben Fraj, A.; Barthélémy, J.-F. Improvement of the compressive strength of recycled aggregate concretes and relative effects on durability properties. *Constr. Build. Mater.* **2023**, *384*, 131447. [\[CrossRef\]](#)

20. Schubert, S.; Hoffmann, C.; Leemann, A.; Moser, K.; Motavalli, M. Recycled aggregate concrete: Experimental shear resistance of slabs without shear reinforcement. *Eng. Struct.* **2012**, *41*, 490–497. [[CrossRef](#)]
21. Zhang, J.; Wang, F.; Zhao, D.; Zhang, M.; Cao, W. Seismic performance of resilient recycled aggregate piloti-type structure employing ultra-high strength bars. *Eng. Struct.* **2023**, *282*, 115795. [[CrossRef](#)]
22. Zhang, J.; Li, C.; Ding, L.; Li, J. Performance evaluation of cement stabilized recycled mixture with recycled concrete aggregate and crushed brick. *Constr. Build. Mater.* **2021**, *296*, 123596. [[CrossRef](#)]
23. Gao, D.; Jing, J.; Chen, G.; Yang, L. Experimental investigation on flexural behavior of hybrid fibers reinforced recycled brick aggregates concrete. *Constr. Build. Mater.* **2019**, *227*, 116652. [[CrossRef](#)]
24. Mohammed, T.U.; Shikdar, K.H.; Awal, M. Shear strength of RC beam made with recycled brick aggregate. *Eng. Struct.* **2019**, *189*, 497–508. [[CrossRef](#)]
25. González, J.S.; Gayarre, F.L.; Pérez, C.L.-C.; Ros, P.S.; López, M.A.S. Influence of recycled brick aggregates on properties of structural concrete for manufacturing precast prestressed beams. *Constr. Build. Mater.* **2017**, *149*, 507–514. [[CrossRef](#)]
26. Visintin, P.; Dadd, L.; Alam, M.U.; Xie, T.; Bennett, B. Flexural performance and life-cycle assessment of multi-generation recycled aggregate concrete beams. *J. Clean. Prod.* **2022**, *360*, 132214. [[CrossRef](#)]
27. Anike, E.E.; Saidani, M.; Olubanwo, A.O.; Anya, U.C. *Flexural Performance of Reinforced Concrete Beams with Recycled Aggregates and Steel Fibres*; Elsevier: Amsterdam, The Netherlands, 2022; pp. 1264–1278.
28. Özkılıç, Y.O.; Başaran, B.; Aksoylu, C.; Karalar, M.; Martins, C.H. Mechanical behavior in terms of shear and bending performance of reinforced concrete beam using waste fire clay as replacement of aggregate. *Case Stud. Constr. Mater.* **2023**, *18*, e02104. [[CrossRef](#)]
29. Wang, J.; Xu, Q. The combined effect of load and corrosion on the flexural performance of recycled aggregate concrete beams. *Struct. Concr.* **2023**, *24*, 359–373. [[CrossRef](#)]
30. Guan, Q.; Yang, M.; Shi, K.; Zhang, T. Experimental Study and Finite Element Analysis on the Flexural Behavior of Steel Fiber Reinforced Recycled Aggregate Concrete Beams. *Materials* **2022**, *15*, 8210. [[CrossRef](#)] [[PubMed](#)]
31. Tang, L.; Liu, T.; Sun, P.; Wang, Y.; Liu, G. Sisal fiber modified construction waste recycled brick as building material: Properties, performance and applications. *Structures* **2022**, *46*, 927–935. [[CrossRef](#)]
32. Saha, A.S.; Amanat, K.M. Rebound hammer test to predict in-situ strength of concrete using recycled concrete aggregates, brick chips and stone chips. *Constr. Build. Mater.* **2021**, *268*, 121088. [[CrossRef](#)]
33. Xiong, B.; Demartino, C.; Xu, J.; Simi, A.; Marano, G.C.; Xiao, Y. High-strain rate compressive behavior of concrete made with substituted coarse aggregates: Recycled crushed concrete and clay bricks. *Constr. Build. Mater.* **2021**, *301*, 123875. [[CrossRef](#)]
34. Meng, T.; Wei, H.; Dai, D.; Liao, J.; Ahmed, S. Effect of brick aggregate on failure process of mixed recycled aggregate concrete via X-CT. *Constr. Build. Mater.* **2022**, *327*, 126934. [[CrossRef](#)]
35. Dang, J.; Xiao, J.; Duan, Z. Effect of pore structure and morphological characteristics of recycled fine aggregates from clay bricks on mechanical properties of concrete. *Constr. Build. Mater.* **2022**, *358*, 129455. [[CrossRef](#)]
36. *ACI-Committee 408; Bond and Development of Straight Reinforcing Bars in Tension*. American Concrete Institute: Farmington Hills, MI, USA, 2003.
37. Lopez, J.E.; Paz, S.S.; Fonteboia, B.G.; Abella, F.M. Bond behavior of recycled concrete: Analysis and prediction of bond stress-slip curve. *J. Mater. Civ. Eng.* **2017**, *29*, 04017156. [[CrossRef](#)]
38. Harajli, M.H. Comparison of Bond Strength of Steel Bars in Normal- and High-Strength Concrete. *J. Mater. Civ. Eng.* **2004**, *16*, 365–374. [[CrossRef](#)]
39. Zuo, J.; Darwin, D. Splice strength of conventional and high relative rib area bars in normal and high-strength concrete. *ACI Struct. J.* **2000**, *97*, 630–641.
40. Esfahani, R.; Rangan, V. Bond between normal strength and high-strength concrete (HSC) and reinforcing bars in splices in beams. *ACI Struct. J.* **1998**, *95*, 272–280.
41. Azizinamini, A.; Stark, M.; Roller, J.J.; Ghosh, S.K. Bond performance of reinforcing bars embedded in high-strength concrete. *ACI Struct. J.* **1993**, *95*, 554.
42. Prince, M.J.R.; Singh, B. Bond behaviour of deformed steel bars embedded in recycled aggregate concrete. *Constr. Build. Mater.* **2013**, *49*, 852–862. [[CrossRef](#)]
43. Zheng, Y.; Xiao, Y. A comparative study on strength, bond-slip performance and microstructure of geopolymer/ordinary recycled brick aggregate concrete. *Constr. Build. Mater.* **2023**, *366*, 130257. [[CrossRef](#)]
44. Zhang, H.; Geng, Y.; Wang, Y.-Y.; Li, X.-Z. Experimental study and prediction model for bond behaviour of steel-recycled aggregate concrete composite slabs. *J. Build. Eng.* **2022**, *53*, 104585. [[CrossRef](#)]
45. Hoque, M.; Islam, N.; Islam, M.; Kader, M.A. Bond behavior of reinforcing bars embedded in concrete made with crushed clay bricks as coarse aggregates. *Constr. Build. Mater.* **2020**, *244*, 118364. [[CrossRef](#)]
46. *ACI 318-19; Building Code Requirements for Structural Concrete and Commentary*. American Concrete Institute: Farmington Hills, MI, USA, 2019.
47. Sulaiman, M.F.; Ma, C.-K.; Apandi, N.M.; Chin, S.; Awang, A.Z.; Mansur, S.A.; Omar, W. A Review on Bond and Anchorage of Confined High-strength Concrete. *Structures* **2017**, *11*, 97–109. [[CrossRef](#)]
48. Darwin, D.; Tholen, M.L.; Idun, E.K.; Zuo, J. Development length criteria for conventional and high relative rib area reinforcing bars. *ACI Struct. J.* **1996**, *93*, 347–359.

49. Yerlici, V.; Ozturan, T. Bond Properties in High-Strength Concrete Elements. *Digest* **2001**, *13*, 745–769.
50. Dang, J.; Zhao, J. Influence of waste clay bricks as fine aggregate on the mechanical and microstructural properties of concrete. *Constr. Build. Mater.* **2019**, *228*, 116757. [[CrossRef](#)]
51. Zheng, C.; Lou, C.; Du, G.; Li, X.; Liu, Z.; Li, L. Mechanical properties of recycled concrete with demolished waste concrete aggregate and clay brick aggregate. *Results Phys.* **2018**, *9*, 1317–1322. [[CrossRef](#)]
52. Riaz, M.R.; Hameed, R.; Ilyas, M.; Akram, A.; Siddiqi, Z.A. Mechanical Characterization of Recycled Aggregate Concrete. *Pak. J. Eng. Appl. Sci.* **2015**, *16*, 25–32.
53. Momeni, E.; Omidinasab, F.; Dalvand, A.; Goodarzimehr, V.; Eskandari, A. Flexural Strength of Concrete Beams Made of Recycled Aggregates: An Experimental and Soft Computing-Based Study. *Sustainability* **2022**, *14*, 11769. [[CrossRef](#)]
54. Ignjatović, I.S.; Marinković, S.B.; Mišković, Z.M.; Savić, A.R. Flexural behavior of reinforced recycled aggregate concrete beams under short-term loading. *Mater. Struct.* **2013**, *46*, 1045–1059. [[CrossRef](#)]
55. Singh, A.; Miao, X.; Zhou, X.; Deng, Q.; Li, J.; Zou, S.; Duan, Z. Use of recycled fine aggregates and recycled powders in sustainable recycled concrete. *J. Build. Eng.* **2023**, *77*, 107370. [[CrossRef](#)]
56. Xu, Z.; Zhu, Z.; Zhao, Y.; Guo, Z.; Chen, G.; Liu, C.; Gao, J.; Chen, X. Production of sustainable plastering mortar containing waste clay brick aggregates. *Case Studies in Construction. Materials* **2022**, *16*, e01120.
57. Likes, L.; Markandeya, A.; Haider, M.M.; Bollinger, D.; McCloy, J.S.; Nassiri, S. Recycled concrete and brick powders as supplements to Portland cement for more sustainable concrete. *J. Clean. Prod.* **2022**, *364*, 132651. [[CrossRef](#)]
58. ASTM C127 Standard Test Method for Relative Density (Specific Gravity) and Absorption of Coarse Aggregate. 2015. Available online: <https://www.astm.org/c0127-15.html> (accessed on 1 February 2023).
59. ASTM C128 Standard Test Method for Relative Density (Specific Gravity) and Absorption of Fine Aggregate. 2022. Available online: <https://www.astm.org/c0128-22.html> (accessed on 1 February 2023).
60. ASTM C29 Standard Test Method for Bulk Density ('Unit Weight') and Voids in Aggregate. 2017. Available online: https://www.astm.org/c0029_c0029m-17a.html (accessed on 28 January 2023).
61. *B. Standard BS 812-110*; 1990 Testing Aggregates-Part 110: Methods for Determination of Aggregate Crushing Value (ACV). BSI: London, UK, 1990.
62. *BS 812: 112*; Testing Aggregates—Part 112, Methods for Determination of Aggregate Impact Value. British Standards Institution: London, UK, 1990.
63. Choi, K. Anchorage of Beam Reinforced at Conventional and Fibrous Beam-Column Connections. Ph.D. Thesis, Michigan State University, East Lansing, MI, USA, 1988.
64. Hameed, R.; Turatsinze, A.; Duprat, F.; Sellier, A. Bond stress-slip behaviour of steel reinforcing bar embedded in hybrid fiber-reinforced concrete. *KSCE J. Civ. Eng.* **2013**, *17*, 1700–1707. [[CrossRef](#)]
65. *ASTM C642-21*; Standard Test Method for Density, Absorption, and Voids in Hardened Concrete. ASTM: West Conshohocken, PA, USA, 2022.
66. *C. Astm 39*; Standard Test Method for Compressive Strength of Cylindrical Concrete Specimens. ASTM International: West Conshohocken, PA, USA, 2001.
67. *A.440 Committee ACI 440.3 R-04*; Guide Test Methods for Fiber-Reinforced Polymers (FRPs) for Reinforcing or Strengthening Concrete Structures. American Concrete Institute: Farmington Hills, MI, USA, 2004.
68. Nasr, M.S.; Salman, A.J.; Ghayyib, R.J.; Shubbar, A.; Al-Mamoori, S.; Al-Khafaji, Z.; Hashim, T.M.; Hasan, Z.A.; Sadique, M. Effect of Clay Brick Waste Powder on the Fresh and Hardened Properties of Self-Compacting Concrete: State-of-the-Art and Life Cycle Assessment. *Energies* **2023**, *16*, 4587. [[CrossRef](#)]
69. *A. S. Australian Standard AS 3600*; Australian Standard for Concrete Structures. Concrete Structures. Standards Association of Australia: North Sydney, Australia, 2009.
70. *CEB-FIP Model Code 2010*; Model Code Prepared by Special Activity Group 5. CEB-FIP: Lausanne, Switzerland, 2010.
71. Seara-Paz, S.; González-Fontebo, B.; Eiras-López, J.; Herrador, M.F. Bond behavior between steel reinforcement and recycled concrete. *Mater. Struct.* **2014**, *47*, 323–334. [[CrossRef](#)]
72. Kim, S.-W.; Yun, H.-D. Influence of recycled coarse aggregates on the bond behavior of deformed bars in concrete. *Eng. Struct.* **2013**, *48*, 133–143. [[CrossRef](#)]

Disclaimer/Publisher's Note: The statements, opinions and data contained in all publications are solely those of the individual author(s) and contributor(s) and not of MDPI and/or the editor(s). MDPI and/or the editor(s) disclaim responsibility for any injury to people or property resulting from any ideas, methods, instructions or products referred to in the content.